NASA CONTRACTOR REPORT

SPECTROGRAPHIC STUDIES: ELECTRON-INDUCED LUMINESCENCE IN OPTICAL MATERIALS

by John Romanko, J. K. Miles, and P. R. Cheever

Prepared by
GENERAL DYNAMICS
CONVAIR AEROSPACE DIVISION
Fort Worth, Texas
for Langley Research Center

NATIONAL AERONAUTICS AND SPACE ADMINISTRATION • WASHINGTON, D. C. • DECEMBER 1971

1. Report No.	2. Government Accession No.	3. Recipient's Catalog No.
NASA CR-1921		

4. Title and Subtitle	5. Report Date
SPECTROGRAPHIC STUDIES: ELECTRON-INDUCED LUMINESCENCE IN OPTICAL MATERIALS	December 1971
	6. Performing Organization Code

7. Author(s)	8. Performing Organization Report No.
John Romanko, J. K. Miles, and P. R. Cheever	FZK-376
	10. Work Unit No.

9. Performing Organization Name and Address	11. Contract or Grant No.
General Dynamics Convair Aerospace Division Fort Worth, Texas	Contract No. NAS1-7734
	13. Type of Report and Period Covered Contract Report - April 15,1969 to April 15, 1971

12. Sponsoring Agency Name and Address	14. Sponsoring Agency Code
National Aeronautics and Space Administration Washington, D.C. 20546	

15. Supplementary Notes

This report supplements material presented in SPECTROGRAPHIC STUDIES OF LUMINESCENCE IN CHARGED-PARTICLE-IRRADIATED OPTICAL MATERIALS, NASA CR-66758, March 21, 1969.

16. Abstract

The spectral luminescence induced in uv grade sapphire, MgF_2 and LiF_2, three fused silicas and three Corning "glasses," by 1/2, 1, 2, and 3 MeV electrons at fluences from 6.63×10^{10} to 5.30×10^{12} e/cm^2-sec was recorded in the wavelength range from the LiF uv cutoff to the near visible utilizing a plane-grating spectrograph with photographic recording at resolutions of 0.8 and 1.6 nm. Qualitative results based on relative density tracings of seven of the nine materials obtained from preliminary plates are given; quantitative results await calibration and data reduction of the forty final plates.

17. Key Words (Suggested by Author(s))	18. Distribution Statement
Spectrographic studies Luminescence Electron-induced luminescence Optical materials Radiation effects in optical materials	Unclassified - Unlimited

19. Security Classif. (of this report)	20. Security Classif. (of this page)	21. No. of Pages	22. Price*
Unclassified	Unclassified	65	$3.00

*For sale by the National Technical Information Service, Springfield, Virginia 22151

TABLE OF CONTENTS

LIST OF FIGURES

SPECTROGRAPHIC STUDIES: ELECTRON-INDUCED LUMINESCENCE IN OPTICAL MATERIALS

By John Romanko, J. K. Miles, and P. R. Cheever
GENERAL DYNAMICS
Convair Aerospace Division
Fort Worth Operation

SUMMARY

An experimental investigation was conducted to measure the luminescence induced by high-energy electrons in uv-transmitting face plate materials for optical instruments. Spectral luminescence was recorded in the uv wavelength range from the lithium fluoride cutoff to the near visible at resolutions of 0.8 nm and 1.6 nm utilizing a high-aperture plane-grating spectrograph. Electron irradiations were performed at energies of 1/2, 1, 2 and 3 MeV at fluxes from 6.63×10^{10} to 5.30×10^{12} electrons/cm^2-sec. Line spectra characteristic of excited silicon, aluminum, boron, and lead were observed in electron-irradiated Corning 7740. All other samples showed only continuous luminescence. Preliminary spectral density plots show that the induced continuous luminescence covers the range from approximately the short wavelength transmission limit of each material to the visible region, decreasing in total intensity by material in the following order: sapphire, LiF, MgF_2, fused silicas, and Corning glasses. The absolute spectral luminescence intensity as a function of various electron beam and sample parameters awaits calibration and data reduction of the final spectroscopic plates. A 38 Ci Sr^{90}-Y^{90} Čerenkov uv radiation source was designed and fabricated for use in these calibrations.

INTRODUCTION

Transparent optical materials find a variety of applications in space missions: the bulk materials are used as refractive components of navigational control systems such as star trackers, as windows of photomultiplier tubes, and as camera lenses. The thin film materials are used as transparent protective covers for solar cells and reflective optics of telescopes and other scientific instruments.

The program described herein was initiated with the objective of conducting an experimental and analytical program to determine the extent of luminescence induced by high-energy charged particles in the ultraviolet region of the electromagnetic spectrum in uv transmitting optical materials. This was a continuation of a program concerning measurements made in the range from 350 to 650 nm on materials used primarily in the visible region (Ref. 1).

The imperative need for luminescence data in the vacuum ultraviolet region cannot be overemphasized in, for example, the Orbital Astronomical Observatory (OAO) program in which detailed stellar maps of the ultraviolet portion of the electromagnetic spectrum will be obtained (Ref. 2). Since the intensity of the Čerenkov component of luminescence varies as $(\text{wavelength})^{-3}$ (Ref. 3), it will be dominant in the ultraviolet region. Also, with new families of photomultipliers now available with responses down to 120 nm, measurements were desired of the luminescence generated in the ultraviolet wavelength region in typical window materials employed in these new phototubes.

A review of the subject matter available in the open literature prior to initiation of the original program revealed the dearth of practical luminescence data required for adequate selection of optical materials for space application. Although a number of excellent studies have been performed to date (Refs. 4 through 6), as is summarized succinctly in Reference 1, the literature survey showed little information on the general subject of luminescence induced in charged-particle irradiated materials for optical use. Moreover, there are practically no quantitative data reported on the relative contributions of the various mechanisms involved. The limited information available is usually of the "broad band pass" type covering large wavelength intervals, thus obscuring the spectral dependence of the luminescence, and hence the underlying mechanisms.

It is true that a number of studies (Refs. 7 through 9) have been devoted specifically to measuring the luminescence radiation generated in multiplier phototubes of star trackers; however, these data are limited in scope and the luminescence values are not reported in terms of a differential intensity unit (nanowatts/cm^2-steradian-nanometer of wavelength interval). The data generated in this program would be more suitable in predicting the background response of a multiplier phototube subjected to irradiation with charged particles.

The background noise (i.e., anode dark current) arising from the luminescence induced in the face plates and glass envelopes in irradiated multiplier phototubes can severely impair their functioning in a radiation environment. Star trackers can be vulnerable to the indigenous and artificial radiation belts causing the possible critical degradation or complete loss of the control and pointing accuracies of space systems like the OAO. Also, radiation-induced luminescence has probably been responsible for high backgrounds observed from space experiments such as the photometer experiments measuring airglow aboard the second Orbital Geophysical Observatory (OGO-II) (Ref. 9).

The purpose of the program described in this report was manifold:

(1) to measure the spectral distribution of the charged-particle induced luminescence in selected uv transmitting optical materials in the ultraviolet wavelength region in terms of an irradiance standard using a spectrographic technique employing photographic recording;

(2) to determine the dependence of this luminescence radiation on the important parameters describing the charged particles, including particle type, energy and flux, and on the parameters of the irradiated material, including sample type, thickness and temperature;

(3) to deduce, where possible, the relative contributions of the various luminescence mechanisms to aid in describing the response of a multiplier phototube operating in a charged-particle radiation field.

The luminescence mechanisms include the Čerenkov effect, radiative de-excitation of the excited lattice by charged-particle excitation and ionization effects, and radiative de-excitation of excited impurity centers and radiation-induced color centers. A comprehensive treatment of these various luminescence phenomena occurring in charged-particle-irradiated transparent optical materials is given in Reference 10.

It was deemed desirable to thermostat and monitor the temperature of the irradiated samples in order to control and study possible thermal annealing phenomena. As is apparent from an analysis of the data obtained in the visible wavelength region on

ambient samples (Ref. 1), a number of unexplained anomalies could be generally attributed to temperature effects in the irradiated samples.

It was also desirable to conduct irradiations at flux levels lower than used in the visible program in order to establish the relationship between data obtained in accelerated tests to those obtained in tests simulating more closely the expected dose rates in space. Lower dose rates would also reduce the heating effect in the samples.

The usefulness of the data in any practical design consideration can be greatly expanded by irradiating the samples at energies less than 1 MeV, the low-energy limit used in the visible program. Extending the energy range down to 0.5 MeV would yield data more representative of the particle energies of interest to the OAO program, for example.

The materials investigated were Spectrosil B; Suprasil II; uv grade sapphire, MgF_2, and LiF; and Corning types 9741, 7056, 7740 and 0080.

The luminescence radiation intensities of the above materials, after calibration and data reduction of the final plates, will be reported in units of nanowatts/cm^2-steradian-nanometer of wavelength interval. The charged particles are electrons of energies ½, 1, 2 and 3 MeV, at fluxes up to 5.3×10^{12} e/cm^2-sec.

Specific recommendations are presented concerning calibration and data reduction of the final plates and for additional experimental studies designed to extend the measurements into the infrared wavelength region.

SPECTROGRAPHIC TECHNIQUE FOR LUMINESCENCE MEASUREMENTS

The Fort Worth operation has pioneered in the area of the spectrographic method of recording spectral data on luminescence generated in charged-particle-irradiated transparent optical materials since October 1966 under a company-sponsored study concerning a Jupiter fly-by mission (Ref. 6). Studies by others in this field have been previously limited in scope due to the availability of spectrographs of only low light-gathering-power which would record only intense (line) luminescence radiation. Also, a large number of these utilized monochromator techniques

employing photomultiplier detectors. Examples of the spectrographic and monochromator techniques are given in References 11 through 19, the results of which are summarized in Reference 1.

Since the initiation of the present contract work, the spectrographic technique has been vastly improved and extended in scope culminating in the equipment design described in the next section.

In principle, this technique possesses advantages over other techniques: in the photographic recording mode, no electronic equipment is used and the direct photographic record is permanent and ready for analysis by the relatively simple technique of densitometry. If the bremsstrahlung produced by the sample in the electron beam is not too intense, resultant fogging of the photographic emulsion is not of any consequence and the luminescence produced in the sample by the high-energy charged particles will be recorded over this background.

Luminescence data is obtainable in situ, during the irradiation of the optical sample, at which time the photon emission is at its maximum.

The luminescence data so-obtained is spectral data, yielding intensity of luminescence versus wavelength over a large range covering the ultraviolet, visible and near infrared regions; the spectral range recorded is limited only by the spectral response limits of the optics of spectrograph and by the limits of sensitivity of the photographic emulsions of the spectroscopic plates.

This spectrographic technique permits analysis of structure in the spectra to determine the luminescing species and the relative contributions of various processes contributing to the luminescence, including:

(i) the Čerenkov effect (not "luminescence," per se)

(ii) direct electronic excitation and ionization of lattice atoms by high-energy charged particles and the subsequent de-excitation of the excited species,

(iii) excitation and subsequent de-excitation of color centers produced by the incident charged particles, and

(iv) excitation and subsequent de-excitation of impurity centers by the incident charged particles.

UV EXPERIMENTAL CONFIGURATION

The equipment developed in this program is displayed in two photographs (Figs. 1 and 2) showing the two experimental setups, the 0° configuration and the θ_C configuration, respectively, using the 4-MeV Van de Graaff at NASA Langley Research Center's Materials Radiation Laboratory (NASA/LRC MRL). A schematic diagram of the two configurations is shown in Figure 3.

In either configuration, the four major components of the system, consisting of the Van de Graaff beam tube, the sample chamber, the transfer optics chamber, and the grating spectrograph, are rigidly interconnected to ensure precise alignment of the optical elements at all times. This alignment was periodically monitored with the aid of a low-power (1/2 mW) He-Ne laser through the recording end of the spectrograph. The back of the sample, upon which the charged particle beam impinges, is focused by the single spherical mirror, of 25 cm focal length, onto the slit of the spectrograph at unit magnification so that illumination is viewed from a solid angle of the sample corresponding to the aperture of the spectrograph.

The Van de Graaff beam tube, sample irradiation chamber, transfer optics chamber, and spectrograph are interconnected with appropriate pneumatically-operated gate valves and liquid-nitrogen-trapped oil-diffusion pumps to ensure contamination-free operation of the optical elements during luminescence runs. This arrangement also permits electron beam forming, defining, and flux calibration at the sample position using the rotatable faraday cup and beam-defining aperture in the sample chamber.

Separate vacuum pumps are provided for each major component to permit component isolation such as during installation of specimens and spectroscopic plates into the sample chamber and spectrograph, respectively. Vacuum pumping of the entire system is necessary to permit recording of the luminescence in the ultraviolet wavelength region. The various 2-in. and 4-in. oil diffusion pumps are outfitted with liquid nitrogen traps, and their mechanical forepumps with molecular sieve traps, to minimize oil contamination of the optical components of the spectrograph, transfer optics mirror and sample specimens. All

NASA Photograph L-70-1465

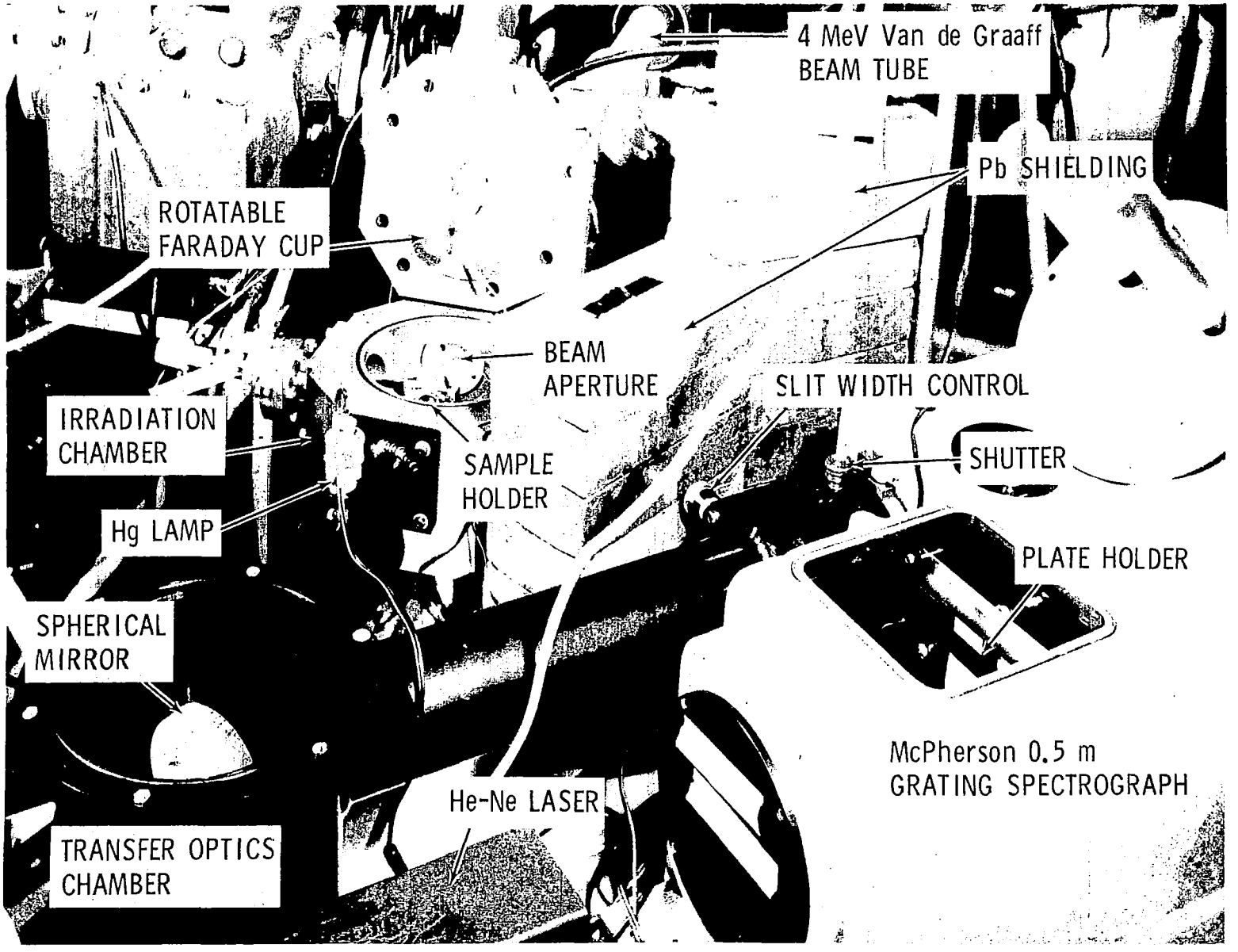

Figure 1 Electron Irradiation-Luminescence Experiments: 0^{o} Configuration

NASA Photograph L-70-2816

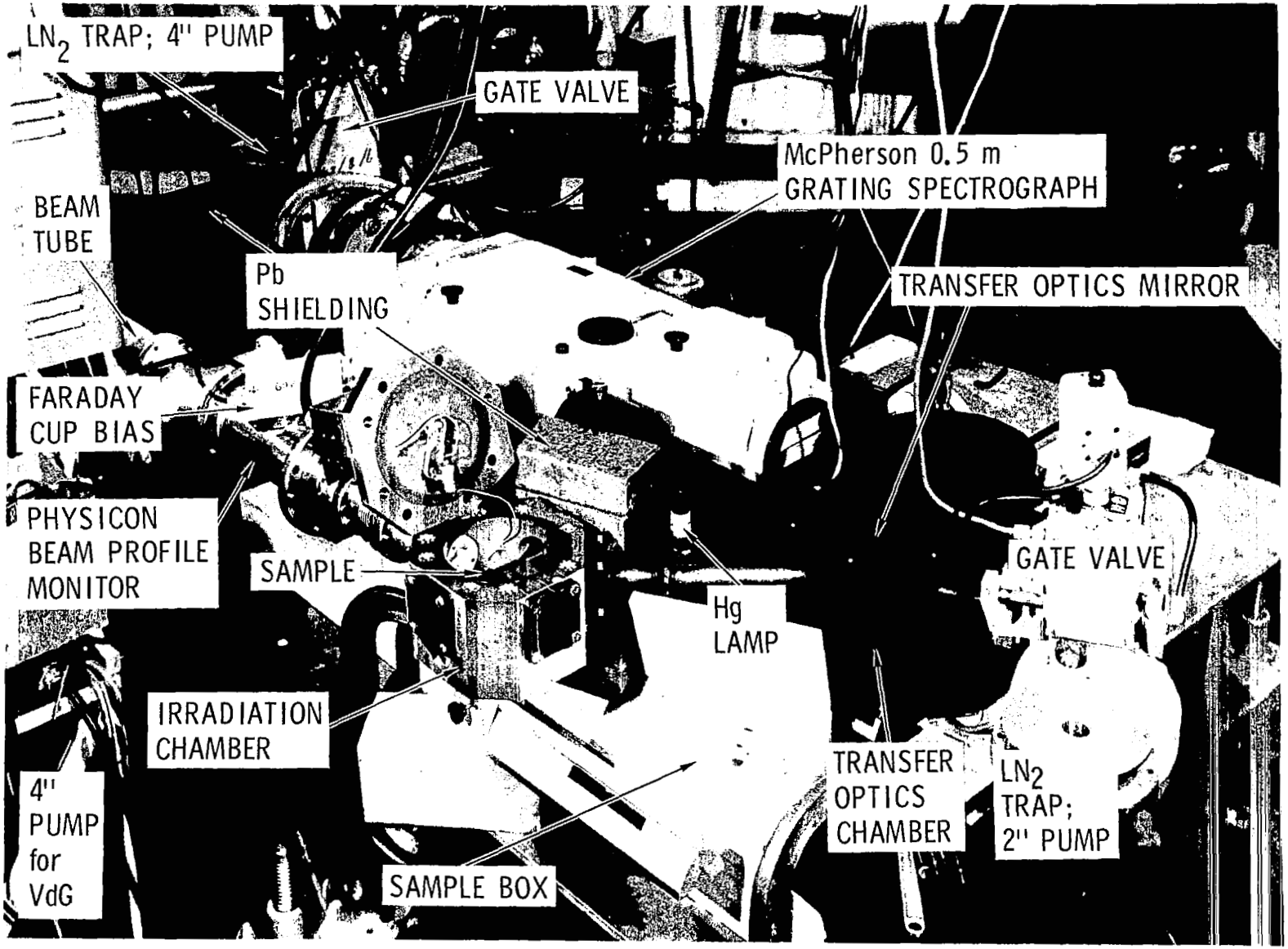

Figure 2 Electron Irradiation-Luminescence Experiments: θ_γ Configuration

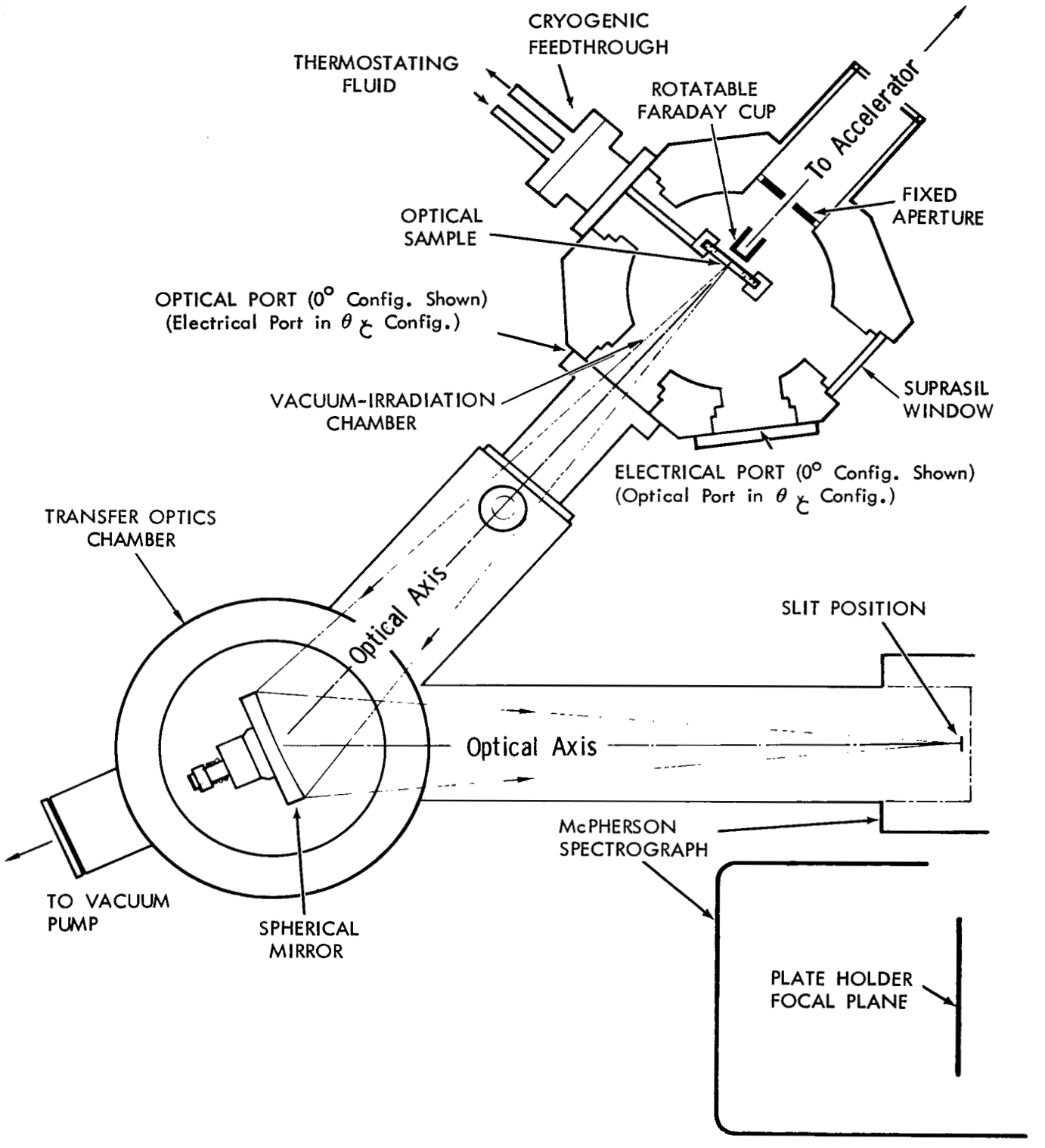

Figure 3 Experimental Configurations

reflective optical components are overcoated with MgF_2 for maximum optical reflectivity in the ultraviolet wavelength region.

The entire system was kept under vacuum during experiments with the uv transmitting materials, such as MgF_2, LiF, sapphire and the fused silicas. In some of the experiments involving the "glass" specimens, such as the Corning types 7056, 7740 and 0080, the spectrograph was operated at atmospheric pressure with the transfer optics chamber-to-spectrograph arm terminated with a MgF_2 window and O-ring to maintain vacuum in the other components. Component sections of the equipment that required servicing were brought to atmospheric pressure from vacuum by slowly admitting Seaford-grade nitrogen to the gate-valve-isolated component, thus maintaining "clean optics" in that section.

A McPherson Model 804/811 4-in. vacuum pumping system with LN_2 trap, was available at Fort Worth to evacuate the spectrograph-transfer optics system for intensity calibration exposures.

The lid of the vacuum-irradiation chamber supports a rotatable Faraday cup available for measurement of the fluxes of ½, 1, 2 and 3 MeV electrons incident on the samples. The Faraday cup is motorized so that it can be rotated in front of the sample during beam flux calibration, and can be rotated out of the irradiation beam during spectrographic recording of the luminescence from the irradiated sample. An insulated fixed beam stop, with a circular aperture of area ¼ cm^2, is located within the neck of the vacuum-irradiation chamber just in front of the rotatable Faraday cup. This arrangement assists in determining the uniformity of the beam on the sample and in monitoring the beam current when the Faraday cup is rotated out of the beam.

A special sample holder was designed to permit circulation of a thermostating fluid for temperature control of the specimens in some of the experiments. A Varian Model V-4540 Variable Temperature Controller unit, with gaseous nitrogen as the working fluid, was used to vary the temperature of the sample holder from approximately -70°F to +100°F. The gas was first cooled by passing it through a copper coil immersed in LN_2. The temperatures were measured with a Brown Electronik multipoint recorder and two copper-constantan thermocouples attached at two points to the sample holder block.

A wall of lead bricks, placed directly between the sample and spectroscopic plate, shields the spectroscopic plate from bremsstrahlung produced in the sample. Additional lead shielding

is judiciously positioned at various places around the spectrograph to minimize background fogging of the photographic emulsion due to stray bremsstrahlung generated at various beam-intercepting components of the Van de Graaff beam transport system.

EQUIPMENT CALIBRATION

Calibration of the various components of the experimental equipment was effected in the following manner.

Optical Alignment

First, the combination of spectrograph, transfer optics mirror, and sample chamber were rigidly mated and optically aligned with a laser beam to ensure that the optical axes of the optical components coincided with the optical axis of the spectrograph. This optical alignment was rechecked periodically during the program, especially after transport of the equipment from one facility to another. Positions of the components of the transfer optics system with respect to the spectrograph slit and sample, respectively, were checked using standard techniques.

The spectrograph used for this work was a McPherson Model 216.5 half-meter plane-grating instrument. Two gratings, each with 600 grooves/mm, were employed giving spectral dispersions of 3.33 nm/mm. These gratings are blazed at 150 nm and 300 nm for high efficiency in the wavelength regions 75 to 225 nm and 150 to 450 nm, respectively. Use was made of 100μ and 200μ slit widths for most of the luminescence recordings, giving resolutions in the first order of approximately 0.8 nm and 1.6 nm, respectively. Slit widths of these magnitudes were found to be optimum, especially in recording the continuous luminescence spectra, without compromising the information recorded on the spectroscopic plates, while at the same time permitting reasonable irradiation and exposure times up to 20 minutes.

Kodak 103aO spectroscopic plates, both uncoated and coated with sodium salicylate, and Kodak SWR spectroscopic plates were used in the recording of the spectral data. The coated plates were prepared by spraying with a 0.5 M methyl alcohol solution of sodium salicylate. The degree of success achieved with each of these emulsions in recording the luminescence is described in another section.

Standard techniques were used in the processing of the spectroscopic plates as recommended by Kodak (Ref. 20).

Charged Particle Dosimetry

Since the Faraday cup could not be in the path of the electron beam during recording of luminescence by the spectrograph, the following dosimetry technique was developed for this "transmission" case. A rotatable Faraday cup was used in conjunction with a fixed beam stop having a circular aperture, concentric with, but smaller in area than the collecting aperture of the Faraday cup. The fixed beam stop with aperture of known area assisted in determining the uniformity of the beam on the sample and in the determination of the flux when the Faraday cup was rotated out of the beam. This was effected by adjusting the electron beam dependent parameters (e.g., gas pressure, steering magnet values, quadrupole focus settings, etc.) until a suitable ratio of current values was obtained for the Faraday cup and beam aperture, viz. i_1 and i_2, respectively. With the Faraday cup rotated out of the beam, the same aperture beam current, i_2, was held constant so that the current falling on the sample, given by $i_2 \times \frac{i_1}{i_2}$, was i_1, as desired.

Beam uniformity of 1, 2 and 3 MeV electrons was monitored spectrographically before and after each series of runs by measuring the degree of uniformity of the density of the photographic image of the spectrograph slit at any given wavelength. In each case the Faraday cup and fixed beam stop were biased at -60 volts to suppress secondary electron emission from the Faraday cup and fixed aperture.

During an actual experiment, the sequence of events was as follows: with the Faraday cup rotated into the beam path, a stable current ratio i_1/i_2 was established such that a specified, uniform, stable flux of charged particles passed through the aperture of the fixed beam stop, corresponding to the current i_1, as registered by the Faraday cup. The Faraday cup was then rotated out of the beam path and a switch was thrown to instantaneously open both the shutter of the spectrograph and a pneumatic gate valve in the beam tube of the charged-particle beam transport system to allow the beam to strike the sample. The current i_2 falling on the fixed aperture stop was integrated with an Elcor Current Indicator and Integrator to a preset integrated current (i.e., integrated flux) corresponding to a desired exposure on the spectroscopic plate emulsion. Upon reaching the preset current value, the Elcor automatically closed both the

shutter of the spectrograph and the pneumatic gate valve of the beam tube, terminating the irradiation exposure.

A current of 10 nA on ¼ cm^2 area of sample, as defined by the fixed aperture, corresponds to a flux of 2.65 x 10^{11} e/cm^2-sec.

Plate Calibration and Data Reduction

Use of the five-step neutral density filter at the sagittal focus position of the spectrograph for plate emulsion calibration in the ultraviolet wavelength region using the standard techniques (see, for example, Ref. 21) would prove unsatisfactory for the true uv transmitting materials, such as uv grade sapphire, LiF, and MgF_2. The reason is that the transmission limits of these materials extends to much shorter wavelengths than the transmission limit of the fused quartz substrate material of the neutral density filter, thus information on luminescence below the fused quartz cutoff would be lost.

Actually, another problem with the neutral density filter arose in an earlier program on visible-transmitting materials (Ref. 1) that precluded the use of the five-step neutral density filter in plate calibration. It was found that the two-mm-high adjacent spectra of the five various intensities overlapped (due to the astigmatic nature of the high aperture grating instrument) to such an extent that microdensitometry of the corresponding images was virtually impossible without introducing large errors in the data. Therefore, various exposure times of the irradiance standard lamp-illuminated Suprasil diffusing screen are made for a convenient spectrograph slit length of 4 mm and the reciprocity law of Bunsen and Roscoe (Ref. 22) is assumed to hold within the allowable experimental error for the range of exposure times used in recording the intensity calibration spectra.

The spectral intensity of the luminescence emitted by an irradiated sample is determined spectrographically by comparing the photographic image of the luminescence spectrum with the photographic images of the spectrum of a known spectral irradiance standard.

In order to eliminate many of the complex problems introduced by the photographic process, the intensity calibration spectrograms are made by duplicating the experimental factors used in the actual luminescence exposures: thus the same optical configuration is used for recording the output of the irradiance

standard as for the luminescence radiation. Also, the calibration exposures are placed on the other half of the plates containing the luminescence exposures.

A Suprasil diffusing screen is placed in the sample holder position and is illuminated uniformly with an irradiance standard located at a known distance. A separate experiment, which involves recording the spectral output at the photographic emulsion with and without the diffusing screen for the same irradiance standard position, determines the "transmission efficiency" factor of the diffusing screen.

Several exposure times of the irradiance standard are selected so that the corresponding photographic densities bracket the densities of the luminescence spectra under calibration. The irradiance standards include a calibrated tungsten iodine-cycle quartz lamp and/or a Sr^{90} Čerenkov radiation source, where necessary. The plates are then developed, fixed and dried en masse according to standard techniques.

The photographic densities of the several spectrograms on each spectroscopic plate are measured with a Joyce, Loebl and Co., Ltd., Model MK IIIC Microdensitometer. For each spectrogram an x-y plot of photographic density (y) versus position (x) on the plate is recorded. Since the dispersion of the spectrograph is very nearly linear, a least squares fit of the positions of several prominent lines of the mercury lamp spectrum are used to correlate the abscissa, x, i.e., the plate position, with the wavelength, λ. Examples of typical luminescence, mercury lamp, and tungsten-iodine lamp spectrogram densitometer traces are presented in Figure 4.

The photographic emulsion is essentially an integrating device whose density of the spectrographic image is a function of the spectral sensitivity of the emulsion and the time integrated intensity. At the same wavelength, when the density of the photographic images of the luminescence and irradiance standard are equal, the exposures are equal, assuming that the reciprocity law of Bunsen and Roscoe (Ref. 22) holds. Thus $D_\lambda^L = D_\lambda^C$, and hence

$$(K_\lambda^L \, I_\lambda^L) \, t^L = (K_\lambda^C \, I_\lambda^C) \, t^C \qquad (1)$$

where L and C refer to the luminescence and calibration data, respectively; D = photographic density; λ = wavelength; K = combined instrument constants; I = intensity; and t = exposure time.

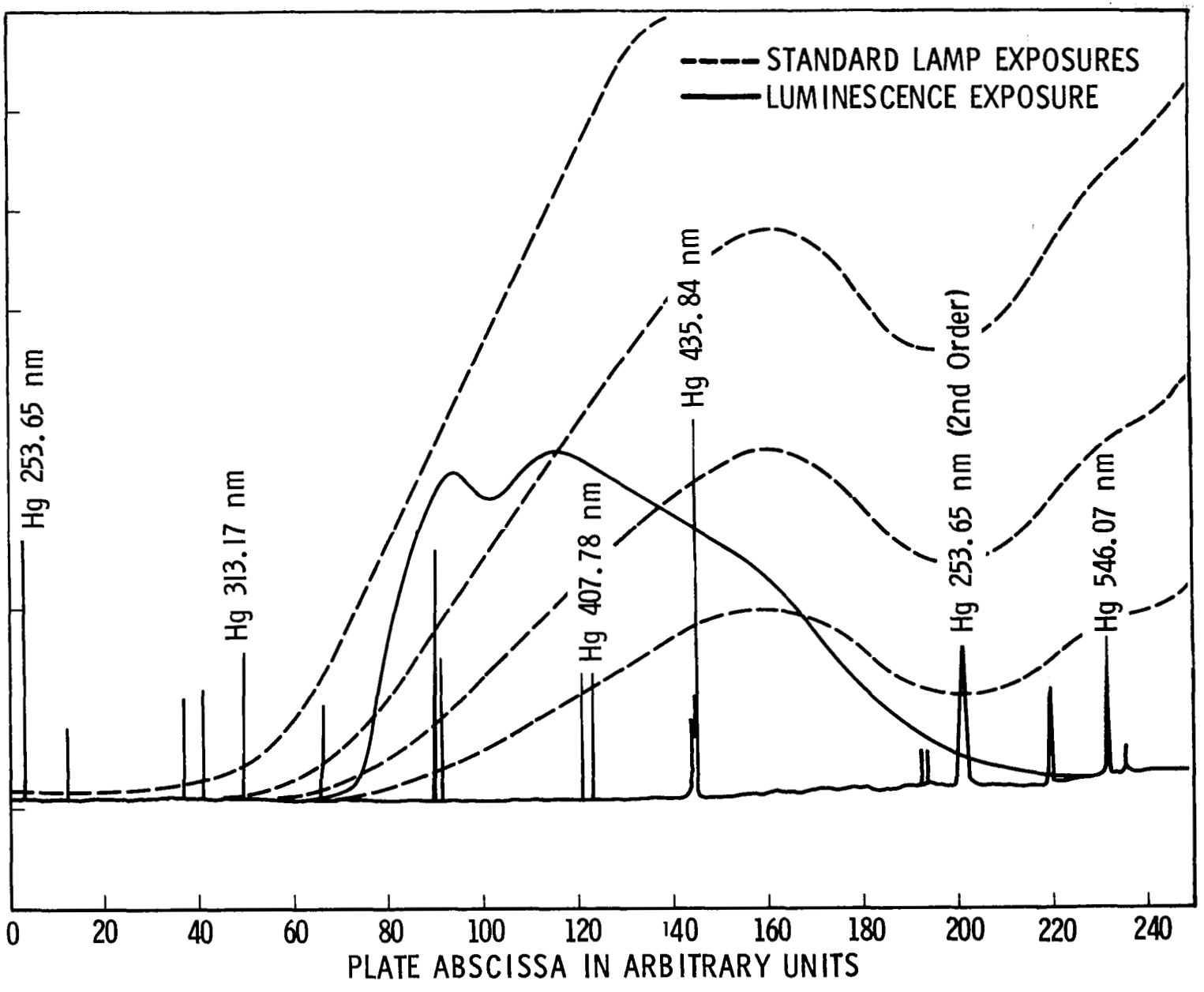

Figure 4 Intensity Calibration of Luminescence

Since the procedure involves a comparison of equal photographic densities between two images, one of which is due to a reference standard, the data (x,y) may be measured from any arbitrary reference as long as all data for a single data reduction set are consistent. This eliminates the necessity for measuring the absolute density above the background fog due to bremsstrahlung.

The constants K_λ^L and K_λ^C are the combined instrument constants, including the spectral reflectivity values of the collimator and camera mirrors of the spectrograph and the transfer optics mirror, and grating efficiency, among others. Since the experimental setup is identical for the luminescence and calibration exposures,

$$K_\lambda^L = K_\lambda^C \ , \tag{2}$$

and

$$I_\lambda^L = I_\lambda^C \frac{t^C}{t^L} \tag{3}$$

Microdensitometer data is obtained for each luminescence exposure and for at least three calibration exposures which bracket the luminescence data. At selected wavelengths (usually at 10 nm intervals) parabolic interpolation of the calibration data (three or more values) is used to determine the exposure time at which the density of a calibration exposure is equal to the luminescence density. An existing digital computer program for the IBM-360 performs the logical operations to select the proper data points for the interpolations, performs the data reduction computations, and prints the absolute luminescence versus wavelength data. These data are used to plot curves of absolute luminescence intensity in units of nW/cm^2-ster-nm as a function of the wavelength, λ, over the wavelength region of interest.

SELECTION OF OPTICAL MATERIALS

Six of the nine types of optical materials used for these studies are those commonly employed in ultraviolet optical devices in space missions (Ref. 2). All nine types are listed in Table I along with the corresponding values of the index of refraction at the wavelength of the NaD lines, and the Čerenkov angle, θ_C.

Up to four thicknesses of a material type were used, e.g. 1/16 in., 0.080 in., 1/8 in., and 1/4 in., to study self-absorption

Table I

OPTICAL MATERIALS FOR LUMINESCENCE STUDIES

Code N_1	Material	uv Cutoff nm	n_D	θ_c^*	Supplier
1	Spectrosil B	170	1.4584	$46^o42'$	Thermal American Fused Quartz Co.
2	Suprasil II	170	1.4584	$46^o42'$	Amersil, Inc.
3	Corning borosilicate 7056	270	1.487	$47^o44'$	Esco Products
4	Corning Pyrex 7740	290	1.474	$47^o17'$	Esco Products
5	Corning lime soda 0080	310	1.512	$48^o36'$	Esco Products
6	Corning uv transmitting 9741	185	1.468	$47^o4'$	RCA
7	Linde uv grade sapphire	145	n_o=1.7681	$55^o33'$	Union Carbide Corp.
8	uv grade lithium fluoride	105	1.3915	$44^o3'$	Harshaw Chemical Co.
9	uv grade magnesium fluoride	113	n_o=1.3777 n_e=1.3895	$43^o28'$ $43^o58'$	Harshaw Chemical Co.

*Obtained using Equation (2) of Appendix A.

effects within the samples of the luminescence radiation generated therein, and, in the case of the thin samples, to be able to define more clearly the energy of the incident electrons within the samples. Use of thin samples limits the scattering of the electrons within the sample, restricting the natural half-breadth of the conic distribution of the Čerenkov radiation, and preserving the "directionality" of the Čerenkov radiation. This allowed a portion of it to be viewed in the θ_C direction to distinguish it from the continuous radiation generated during radiative de-excitation of excited species produced by ionization effects of the incident electron beam.

Identification of a specific sample was facilitated by assigning it to a three digit number, $N_1N_2N_3$. The first number N_1 identifies the sample type, according to the code of Table I. The second number, N_2, gives the sample thickness according to the code: 0, 1, 2, and 3, equal to 1/16 in., 1/8 in., 1/4 in., and 0.080 in., respectively. The last digit, N_3, plus 1, is the sample number in the series. Thus Sample 513 denotes Corning type 0080 of thickness 1/8 in., number 4 in that series.

Where samples could not be obtained in the thicknesses desired for an experiment, e.g., C 9741 samples were available only as 0.021-in. thick discs, combinations of thinner specimens were used to make up the appropriate thickness. The 1 1/2-in. diameter samples were mounted off center in the sample holder and rotated from one irradiation to the next so as to utilize several 1/4 cm^2 circular areas. Prior to irradiation, the samples were cleaned with ethyl alcohol to remove any surface contaminants that might interfere with their optical properties.

In experiments involving the 0^o configuration, the minimum sample thickness used exceeded the range of the electrons in order to avoid direct irradiation of the transfer optics mirror. Thinner samples could be used in the θ_C configuration when conducting experiments at that electron energy since the mirror was not in line with the electron beam.

IRRADIATION EXPERIMENTS

All irradiation-luminescence experiments were conducted at NASA/LRC Materials Radiation Laboratory using the 4 MeV Van de Graaff accelerator. Of the four main attempts, only two resulted in successful data recording sessions using the 0^o and the θ_C configurations in the electron irradiation mode. The planned

proton irradiation-luminescence experiment was terminated after a number of unsuccessful attempts due to equipment and funding problems.

The irradiation experiments were designed to obtain a matrix array of spectral luminescence data for the pertinent parameters describing the incident charged particles and the irradiated samples.

The plan was to obtain the desired luminescence spectra at NASA/LRC MRL on the first half of each of the spectroscopic plates; these would subsequently be calibrated at the Convair Aerospace Division in Fort Worth on the corresponding second half using a suitable irradiance standard. Before this could be done, however, preliminary irradiation-luminescence runs had to be conducted and plates developed at NASA/LRC to determine the ranges of photographic exposure times required to obtain usable photographic emulsion (optical) densities for subsequent data reduction. These exposure times would be a function of sample type and thickness, electron energy and flux, spectrographic slit width, spectroscopic plate emulsion type, and irradiation configuration, among others.

After these suitable exposure times were bracketted, preliminary plates were also taken and developed at NASA/LRC periodically during the course of a series of runs with long spectrographic slit lengths to check beam size and uniformity.

The photographic emulsion types used included Kodak SWR, sodium salicylate-overcoated Kodak 103aO, and (uncoated) Kodak 103aO. The overcoated plates were used in irradiation-luminescence experiments with the true uv transmitting materials when problems arose with the SWR emulsions. Uncoated Kodak 103aO plates were used with the Corning glass types 7056, 7740, and 0080, which are not good uv transmitting materials, per se. Examples of densitometer tracings of spectrograms using each of the three types of emulsions are given in a later section.

The 0^{o} configuration was used primarily for experiments on sample thicknesses greater than the effective range of electrons in the material so as not to directly irradiate the transfer optics mirror. The θ_{C} configuration was used to obtain luminescence data on various sample thicknesses including those exceeding the electron range. Luminescence data obtained on thin samples, coupled with data on the same sample thickness in the 0^{o} configuration, would be used to obtain the relative contribution of the continuous luminescence radiation due to the Čerenkov effect and that due to radiative de-excitation effects.

A separate experiment involving measurement of luminescence of an irradiated specimen of Spectrosil thermostated at various temperatures between -70°F and +100°F was conducted to determine the temperature dependence of the recorded luminescence, if any.

Electron beam currents at energies of 1/2, 1, 2, and 3 MeV varied from 2.5 nA for sapphire to 200 nA for C 0080 over a 1/4 cm^2 area, corresponding to fluxes from 6.63 x 10^{10} e/cm^2-sec to 5.30 x 10^{12} e/cm^2-sec, respectively. These fluxes are an order of magnitude lower than those used in the visible experiments (Ref. 1) and were selected to better simulate fluxes encountered in space applications, in addition to reducing the heating effect in the samples. Photographic exposure times varied from 4 min to 20 min, and the corresponding electron fluences ranged from 7.95 x 10^{13} e/cm^2 (2.5 nA for 20 min) to 1.27 x 10^{15} e/cm^2 (200 nA for 4 min). Thicknesses of optical samples varied from 1/16 in. to 1/4 in.

The luminescence spectra were recorded in situ, i.e., during the time of the actual irradiations, with the start and stop of the spectrographic recordings coinciding with the start and cut-off of the electron beam. An automatic, remote control network of interconnected switches at the Van de Graaff console was used in beam formation and definition, flux measurements at the sample position, pneumatic gate valve control and spectrograph rack and shutter manipulations during the luminescence runs.

Forty spectroscopic plates of Kodak emulsion type 103aO, nineteen of which were overcoated with sodium salicylate, were exposed during this series of runs. Each plate contains an average of seven luminescence spectra. Table II summarizes the matrix of electron currents (i.e., fluxes) and energies in these runs. Data at 1/2 MeV was obtained only for some C 0080 samples, and only after considerable difficulty with beam stability so that experiments with other sample types at this energy had to be abandoned. Information on other parameters, such as irradiation configuration (i.e., 0° or θ_C), sample thickness, and five-step neutral density filter exposures, is recorded in the original Log books.

ČERENKOV ULTRAVIOLET RADIATION SOURCE

A radiation source was needed to serve as an irradiance standard for the calibration of spectroscopic plates in the ultraviolet wavelength region in view of the unsuitability of the

Table II

SUMMARY OF LUMINESCENCE SPECTROGRAMS

Sample Type	Electron Beam Currents, nA*										
	1 MeV			2 MeV				3 MeV			
Spectrosil B	10 (1)	40 (1)		5 (2)	10 (1)	20 (1)	50 (6)	5 (3)	10 (7)	20 (5)	40 (1)
Suprasil II	10 (2)			5 (1)	20 (2)						
Corning 7056	50 (1)	200 (1)		50 (1)	100 (2)	200 (1)		50 (1)	100 (1)		
Corning 7740	50 (1)	200 (1)		50 (1)	100 (1)	200 (1)		50 (2)	100 (1)		
Corning 0080	50 (1)	200 (1)		50 (1)	100 (1)	200 (1)		100 (1)			
	1/2 MeV: 100 (1)	400 (1)									
Corning 9741				100 (2)				50 (1)			
uv grade Sapphire	2.5 (1)	10 (1)		2.5 (2)	10 (1)			2.5 (2)	10 (1)		
uv grade LiF	2.5 (2)	10 (1)		2.5 (1)	10 (2)			2.5 (1)	5 (1)	10 (1)	
uv grade MgF_2	2.5 (2)	10 (6)	40 (1)	2.5 (1)	5 (7)	10 (3)	20 (1)	2.5 (1)	5 (8)	10 (2)	20 (2)

* 1 nA ≡ 2.65 x 10^{10} e/cm^2-sec over 1/4 cm^2 area

( ) = number of spectrograms

tungsten-iodine irradiance standard in this region. The desired characteristics of the radiation source were that the radiation source be a continuum extending from approximately the lithium fluoride uv cutoff into the near visible, that its spectral intensity be comparable in magnitude to that of the luminescence experimentally observed, and that it be extremely stable over long time intervals. One possible light source which could meet these requirements was the Čerenkov radiation produced in a transparent dielectric material by electrons from a radioactive source.

Combining an appropriate radionuclide and transparent dielectric material to create a Čerenkov uv radiation source is not a novel idea. The use of Čerenkov radiation generated in a very pure sample of distilled water as an irradiance standard has been suggested by at least two researchers: in 1953, Greenfield et al (Ref. 17) showed that Čerenkov radiation generated in water bombarded by radium gamma rays and by P^{32} beta rays was convenient for the determination of the spectral sensitivity of photographic emulsions. Likewise, Čerenkov radiation was used by Chizhokova (Ref. 23) as a standard to determine the luminescence yield of solutions bombarded by high-speed electrons. At least one commercial manufacturer, International Chemical and Nuclear Corporation, now advertises a 20 mCi Čerenkov radiation source (Ref. 24) for checking light detection systems, and Oak Ridge National Laboratory (ORNL) will fabricate such sources to specification with some restrictions as in our case. A source of Čerenkov radiation produced by Sr^{90} decay electrons in a quartz disc was installed in the OAO-2 (in orbit since December 1968) to calibrate various photomultipliers in the Wisconsin five filter photometer experiment for measurements in the wavelength region from 120 nm to 420 nm (Ref. 2).

The theory and calculations performed to investigate the feasibility of such a Čerenkov source for spectroscopic plate calibration are presented in Appendix A. Therein it is shown that the most likely source consists of radioactive Sr^{90}-Y^{90} as strontium titanate encapsulated in stainless steel with a transparent dielectric material, such as fused silica, for Čerenkov radiation generation. A Čerenkov source ($\sim$ 1000 Ci of Sr^{90}) meeting the intensity requirements corresponding to photographic densities obtained in the visible experiments (Ref. 1) was deemed unfeasible; however, if the intensity of the luminescence recorded in the Van de Graaff irradiation experiments could be lowered and still provide suitable photographic densities for densitometry and subsequent data reduction, a Čerenkov source of lesser intensity could be utilized. Further calculations indicated that, for the desired source dimensions, the maximum source

strength obtainable was 130 Ci of Sr^{90} as strontium titanate. However, a solid Sr^{90} source from ORNL would consist of microspheres of strontium titanate in an aluminum matrix. The estimated maximum practical source intensity for such a source would be 50 Ci. By using revised calibration techniques, a nominal 50 Ci Sr^{90}-Y^{90} Čerenkov radiation source could be used effectively. Consequently, a source of that strength was ordered from ORNL; the resulting fabricated source had a measured strength of 38 Ci.

Čerenkov Source Design

The Čerenkov source consists of a stainless steel capsule containing 38 Ci of Sr^{90} as strontium titanate ($SrTiO_3$) embedded in an aluminum matrix. Specific details on source construction are shown in Figure 5. The 10-mil window permits beta particle transmission to a transparent dielectric material for generation of Čerenkov radiation.

The Sr^{90}-Y^{90} Čerenkov source was designed and fabricated by the Isotope Sales Dept., ORNL, Oak Ridge, Tennessee. The original source, received five months after issuance of the purchase order, was designed with its 10 mil window welded to the capsule body; this source was found to be contaminated due to leakage at the weld and was returned to ORNL. The second and present source (Fig. 5) was successfully fabricated and delivered to General Dynamics two months later. Its design features an integral window and body and a separate plug which was welded in place to complete encapsulation of the source materials.

The iron and lead shield which houses the source is depicted in Figure 6. The body, cavity and lid are all cylindrical. The single steel pin is welded into the body and fits into a recess in the lid permitting the lid to be swivelled to either side for access to the cavity. Two lifting eyes on opposite sides of the body provide for lifting the 546 lb shield.

Two rigid, U-shaped brackets fit into the shield cavity; one positions the Sr^{90}-Y^{90} source capsule at the bottom center of the cylindrical cavity and the other positions the 1½-in.-diameter, ¼-in.-thick Čerenkov medium over the source window. The latter bracket is easily lifted out for interchange or removal of the transparent dielectric medium.

The 38 Ci Sr^{90}-Y^{90} source is hazardous and safe storage and handling procedures must be exercised. The measured beta dose rate is 1300 rad/hr at one foot from the window. The

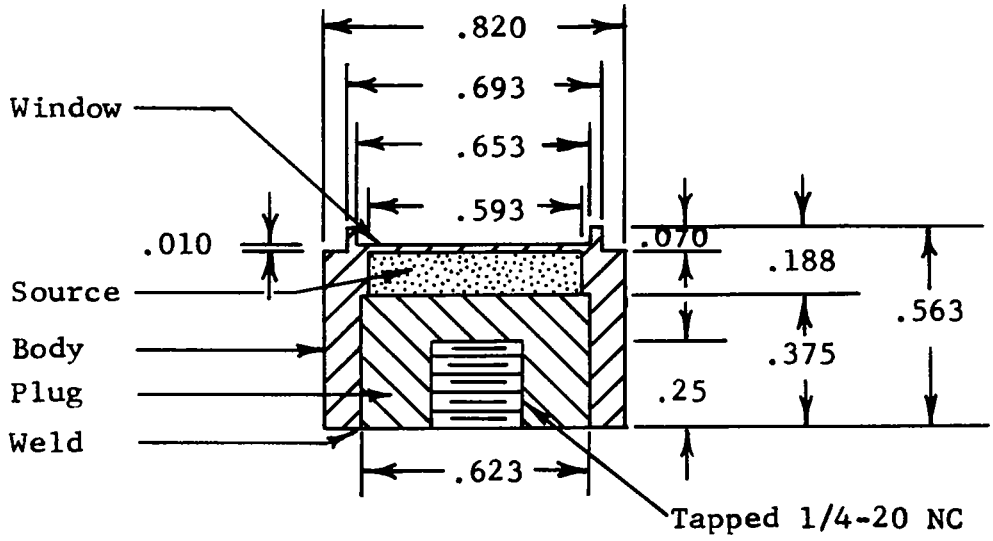

Source: $Sr^{90}TiO_3$ in Aluminum

Capsule: Stainless Steel

Dimensions: Inches

Figure 5 Sr^{90}-Y^{90} Beta Source-Schematic

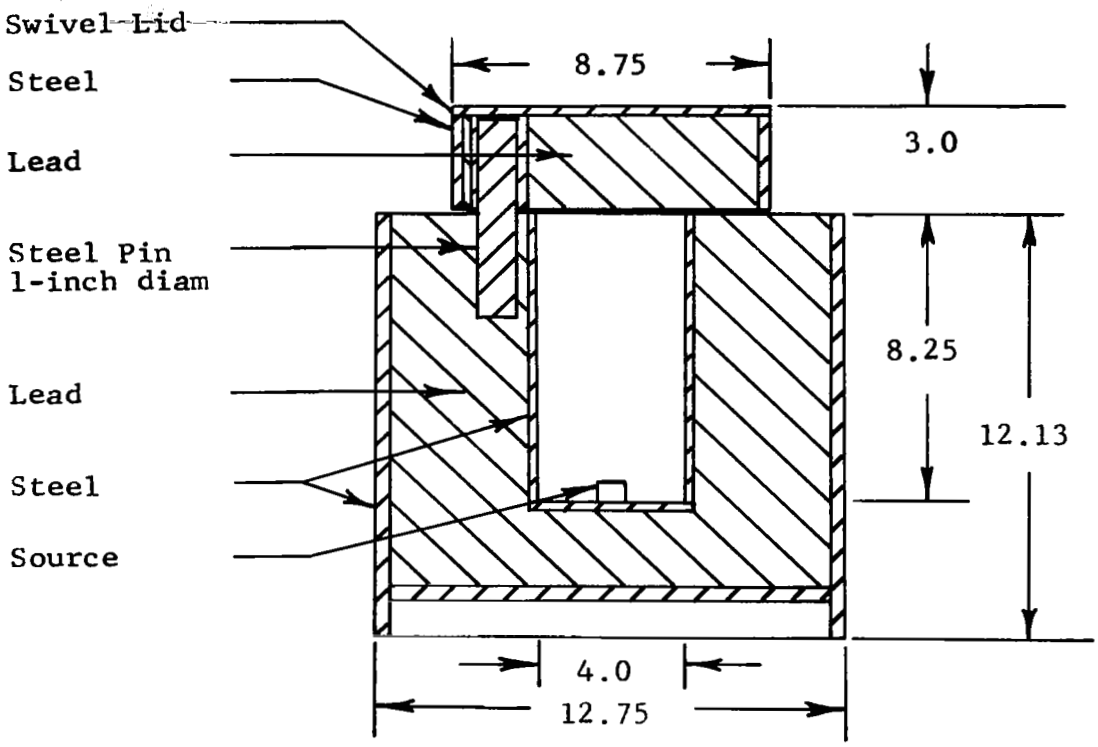

Material: Lead and Steel

Dimensions: Inches

Weight: 546 pounds

Figure 6 Beta Source Shield - Schematic

bremsstrahlung radiation dose rate from total absorption of the beta radiation amounts to approximately 4.5 R/hr at one foot. With the source inside, the dose rate measurements at the top and sides of the closed shield described previously are approximately 2 and 1 mR/hr, respectively. The measurements and hazards are discussed in detail in Appendix A.

Čerenkov Source Calibration

A preliminary calibration of the Sr^{90}-Y^{90} Čerenkov source at one wavelength was accomplished by comparing its intensity to that from a calibrated tungsten-iodine (W-I) irradiance standard as follows: the Sr^{90}-Y^{90} capsule was positioned behind a 1/4-in.-thick Spectrosil B sample at the sample position end of the extended transfer optics chamber arm. Adequate lead shielding was provided to avoid undue exposure to personnel and spectroscopic plates at the recording position. The resultant Čerenkov radiation generated in the Spectrosil was recorded in a 15 min exposure on a Kodak 103a0 plate. Additional exposures were made on the same plate of the calibrated W-I irradiance standard positioned at 40 cm from the sample position at exposure times of 0.5, 2, 8 and 20 min using a slit width 0.4 that used in taking the Čerenkov radiation exposure. A mercury lamp spectrum served for frequency calibration.

Densitometer tracings of the above-mentioned spectrograms are recorded in Figure 7. From these it is noted that densities due to the Čerenkov source and W-I source match at 360 nm, 322.5 nm, 286.5 nm, and 253.7 nm for the 0.5, 2, 8, and 20 min W-I exposures, respectively. Interpolation yields matching intensities for 15 min exposures of both sources at 266.0 nm; applying the inverse square law to the tabulated irradiance value at this distance and wavelength, viz. 2.2×10^{-4} nW/cm^2-nm, and correcting for slit width, yields a Čerenkov radiation source intensity of 8.8×10^{-2} nW/cm^2-nm at 266 nm.

For complete calibration of the Čerenkov uv source it will be necessary to obtain a number of W-I lamp and Čerenkov source spectrograms for different W-I lamp-to-sample separation distances; this will ensure density matches of the two spectra at a sufficient number of different wavelengths to plot a smooth curve over the wavelength range of interest. It was not possible to complete calibration of the source under the existing contract funding restrictions.

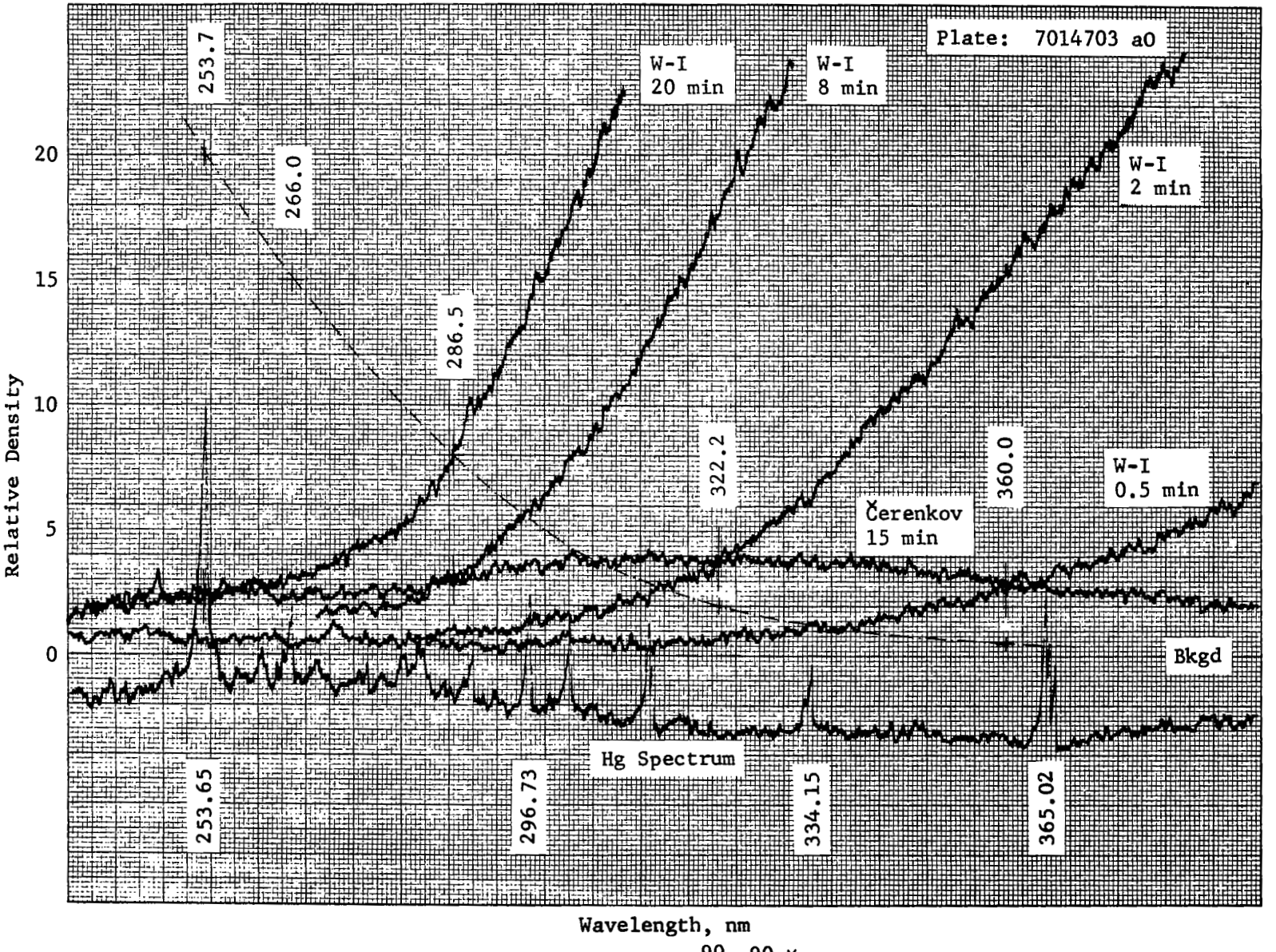

Figure 7 Calibration of Sr^{90}-Y^{90} Čerenkov Source

The Sr^{90}-Y^{90} Čerenkov uv source could also be calibrated by the National Bureau of Standards by a more direct radiometric technique.

Figure 8 records density plots of the luminescence radiation of the Sr^{90}-Y^{90} Čerenkov radiation source after passing through four different neutral density filters at the slit of the spectrograph. Comparison of these with those of Van de Graaff electron-irradiated Spectrosil luminescence (Fig. 9) shows that the spectra are essentially identical. Unfortunately, an overexposed Hg comparison spectrum adjacent to the Čerenkov spectrum obscures details of the latter in the region of the strong Hg line at λ 253.65 nm.

Modified Plate Calibration Procedure

The experimental conditions may be modified in a number of ways to use the 38 Ci Čerenkov source more effectively in spectroscopic plate calibration as follows. Van de Graaff electron irradiations can be conducted at low enough fluxes and photographic exposure times to yield low photographic densities, say less than 2.0, for the recorded spectral luminescence spectrograms. (Those recorded in the visible experiments of Reference 1 resulted in photographic densities as high as 4.0.) Čerenkov calibration spectrograms can be recorded at slit widths of the order of four times those used for recording the Van de Graaff electron-induced luminescence spectra. The resultant densities of the unknown luminescence and Čerenkov calibration source should be suitable to effect the desired densities for data reduction. A separate experiment can be performed to obtain the relationship between density of spectral image on the spectrogram as a function of spectrographic slit width. This relationship should be quite linear for heterochromatic (i.e., continuous) sources (Ref. 25). The calibrated tungsten iodine-cycle irradiance standard can be used for the latter experiment, in addition to serving as an auxiliary standard.

Use of uv grade MgF_2 or sapphire as the Čerenkov medium instead of fused silica will also increase the intrinsic uv intensity of the source, as well as providing a shorter wavelength limit. Use of uv grade LiF as the Čerenkov medium would provide the shortest uv wavelength limit but would create calibration stability problems because of electron-induced absorption bands therein (see p. 46) and the hygroscopic nature of the material. Aluminizing the face of the transparent Čerenkov medium in contact with the Sr^{90}-Y^{90} capsule to provide a second surface

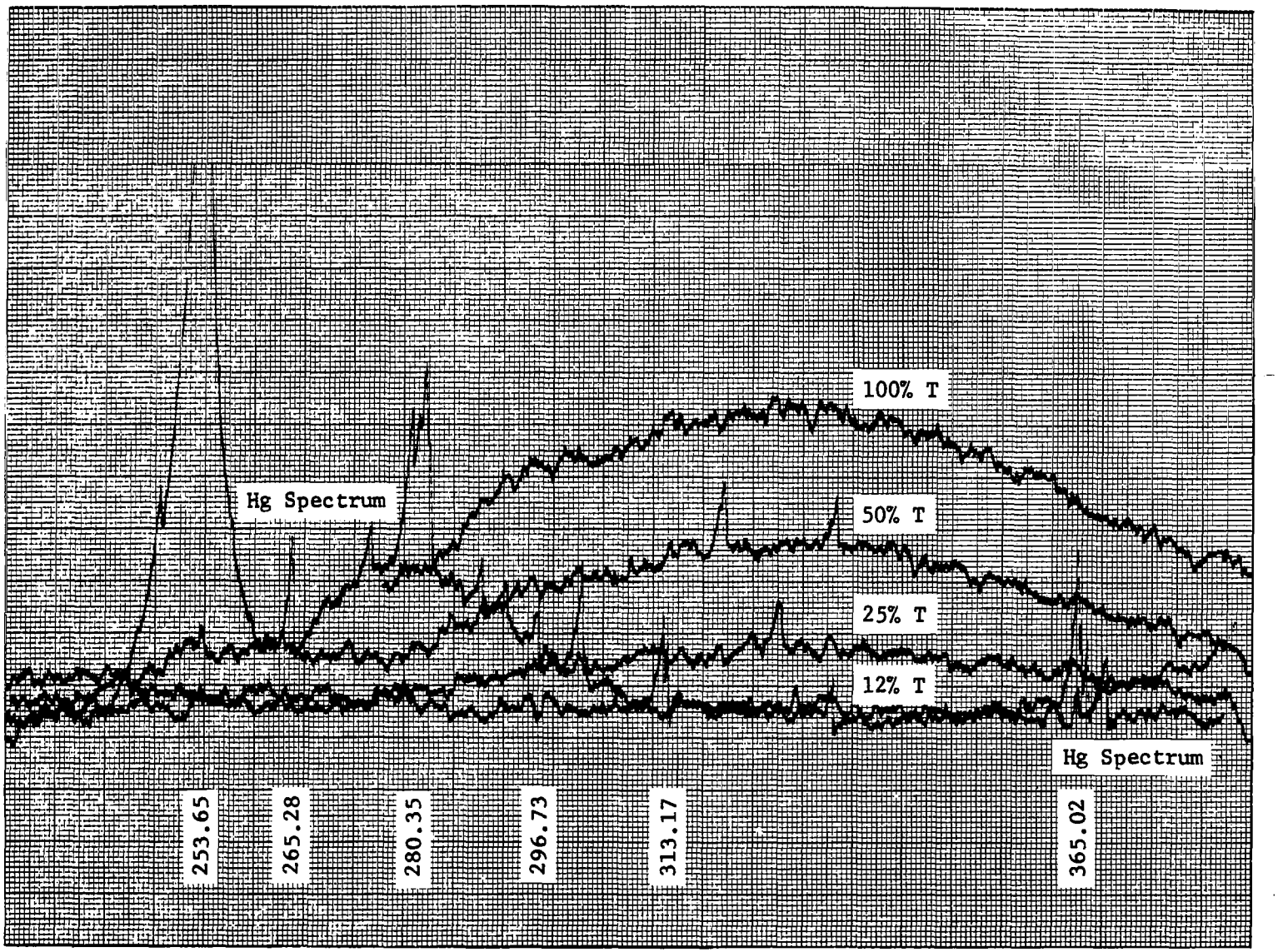

Figure 8 Sr^{90}-Y^{90} Source-Induced Luminescence of Spectrosil B

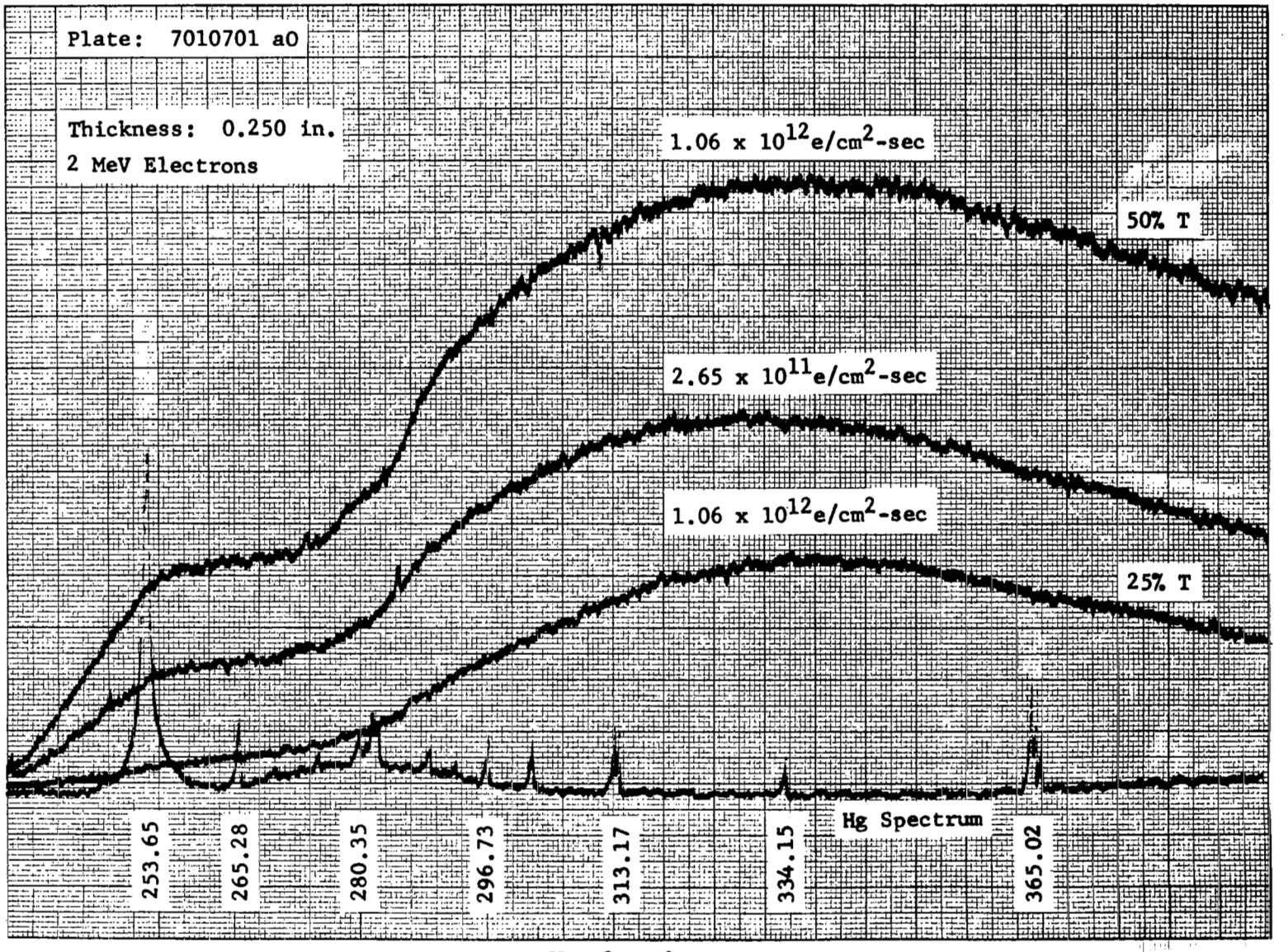

Figure 9 Electron-Induced Luminescence of Spectrosil B

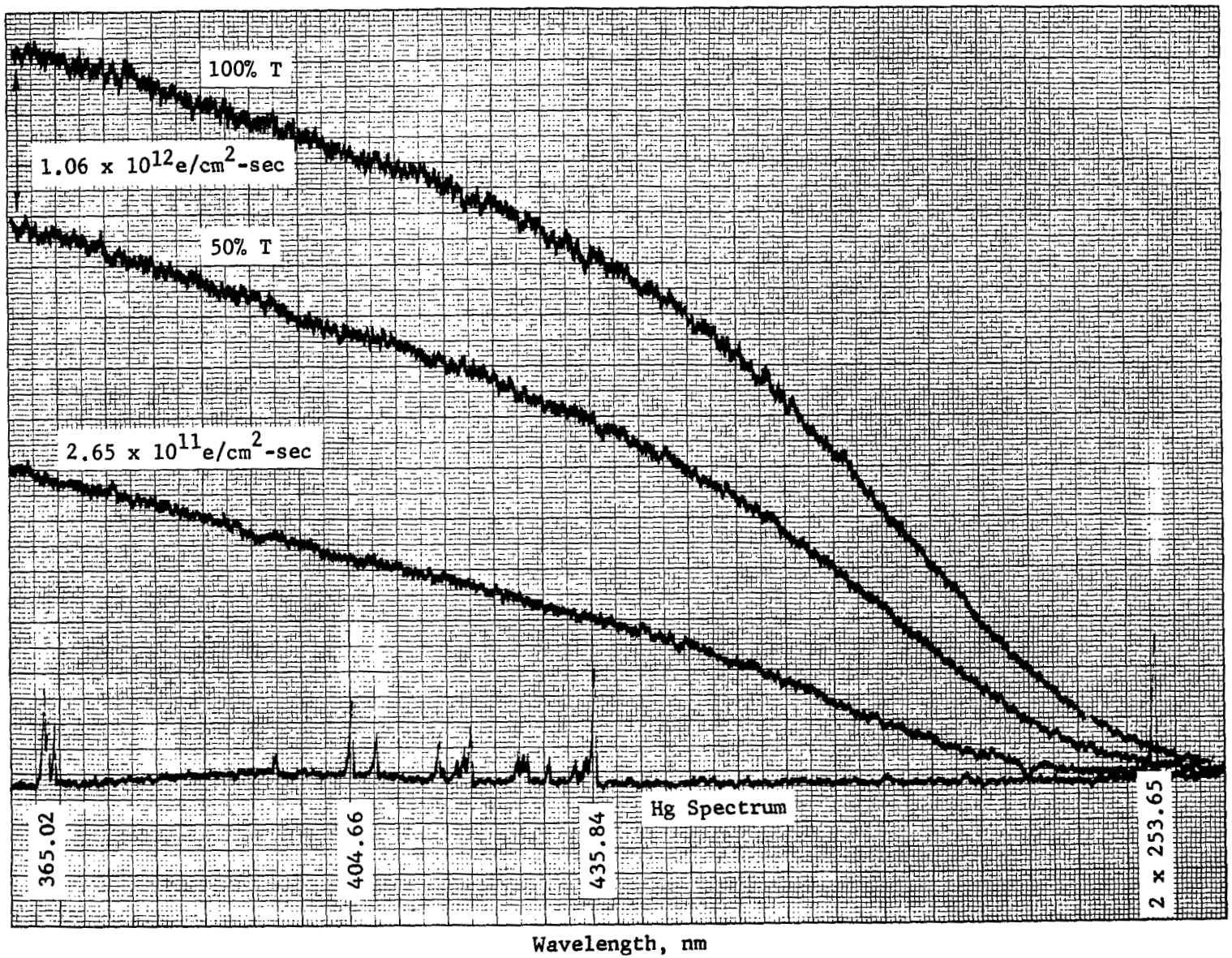

Figure 9 Electron-Induced Luminescence of Spectrosil B (cont'd)

mirror should increase the intensity of the Čerenkov source by approximately a factor of two.

Application of the above modified technique should permit effective use of the 38 Ci Sr^{90}-Y^{90} Čerenkov radiation source in plate calibrations.

RESULTS AND DISCUSSION

Inspection of the spectrograms developed at NASA/LRC MRL to determine suitable exposure times for the final plates reveals that continuous luminescence dominates, with characteristic line spectra appearing in only one of the sample types.

An unexpected problem arose with the first batch of Kodak SWR plates used in the preliminary runs designed to bracket exposure times for suitable plate emulsion densities. This was evidenced by emulsion tearing at the plate edges, emulsion density streaking throughout the plates, and oversize plates in some cases. The supplier (Eastman Kodak Co., Scientific Photography Markets) confirmed these faults after testing the unused plates of this batch, attributing them to manufacturing defects. Since a long lead time was indicated for delivery of a replacement batch, with no guarantee on delivery time or plate emulsion condition, the use of Kodak SWR plates was abandoned in favor of sodium salicylate (NaSal)-overcoated Kodak 103aO plates, as recommended by a number of researchers in uv spectroscopy (Ref. 26).

The short wavelength limit of any plate, e.g., Kodak 103aO, is ultimately governed by the high absorption of the gelatin of the emulsion. Overcoating the plates with Na Sal extends the short wavelength limit of plate emulsion sensitivity by converting the shorter wavelengths by fluorescence to wavelengths to which the gelatin of the emulsion is transparent, and the emulsion itself is sensitive.

Preparation of Na Sal-overcoated plates is simple, according to the procedure of Allison and Burns (Ref. 26), and with its high quantum efficiency (Ref. 27) and essential flatness in response over the region 60 nm to 340 nm (Ref. 28), proved to be useful in the succeeding experiments. The only problem experienced with these plates was the uniform "pitting" of the emulsion at high optical densities resulting in a larger scatter of data in the corresponding densitometer tracings (Figs. 10 and 11).

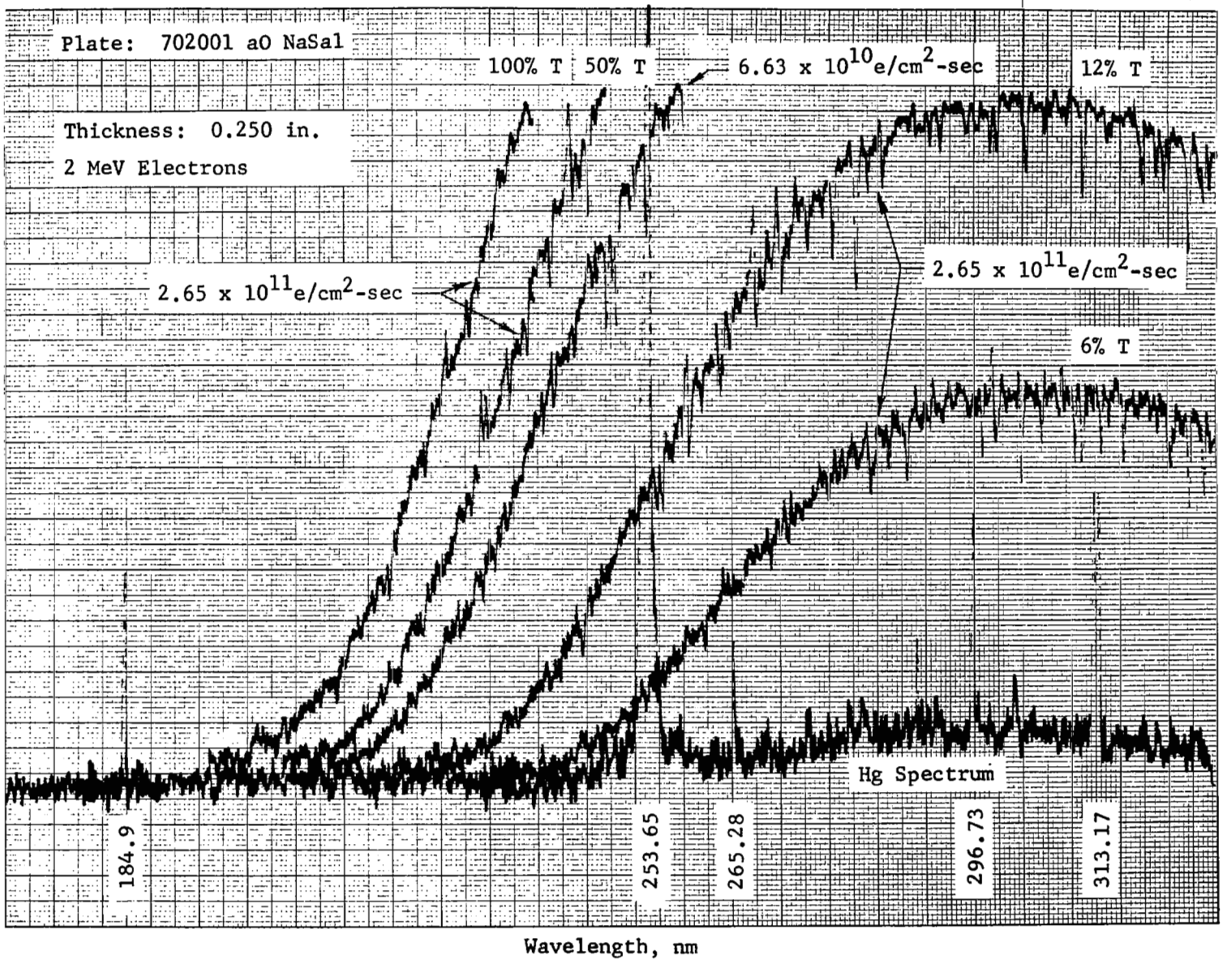

Figure 10 Electron-Induced Luminescence of UV Grade Sapphire

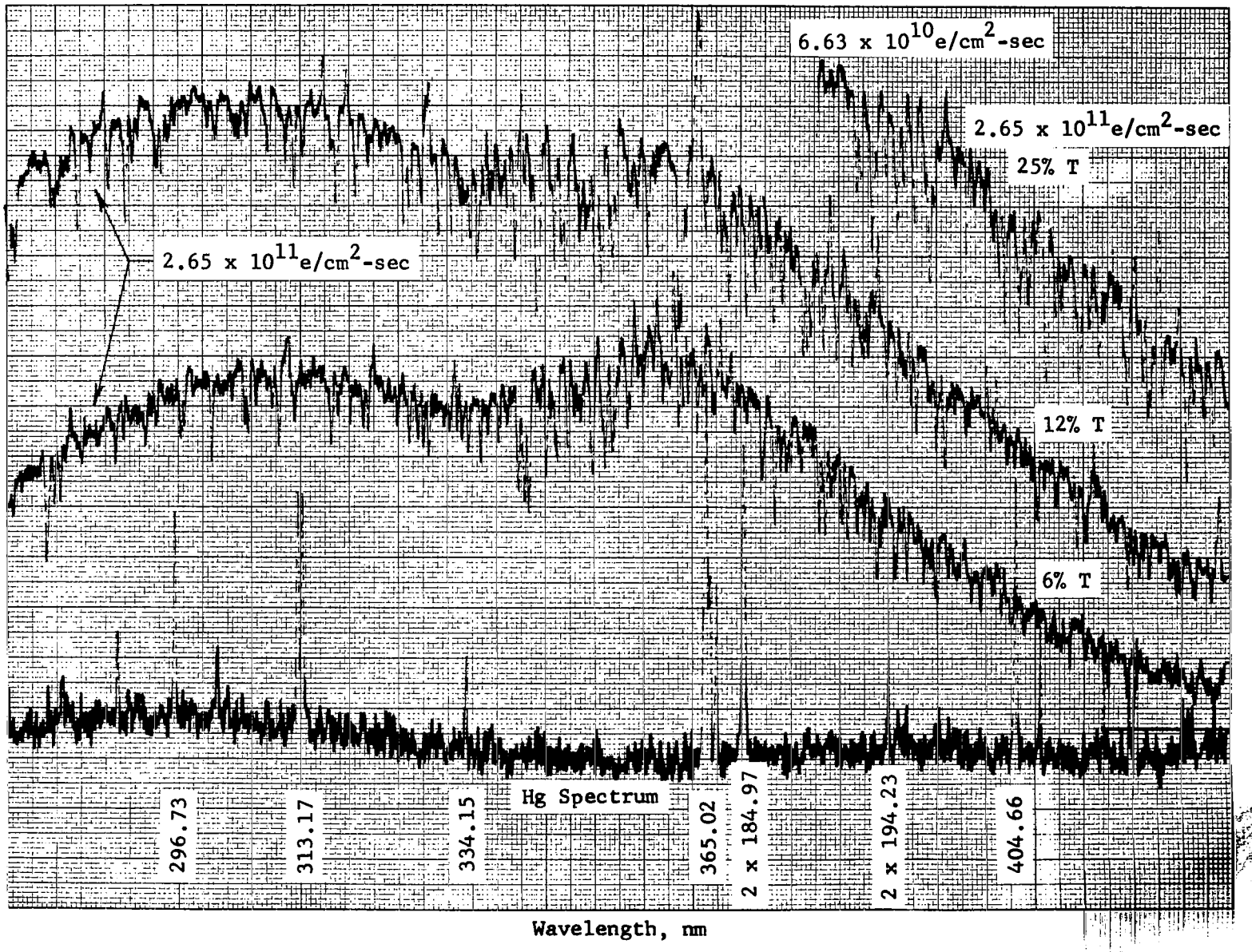

Figure 10 Electron-Induced Luminescence of UV Grade Sapphire (cont'd)

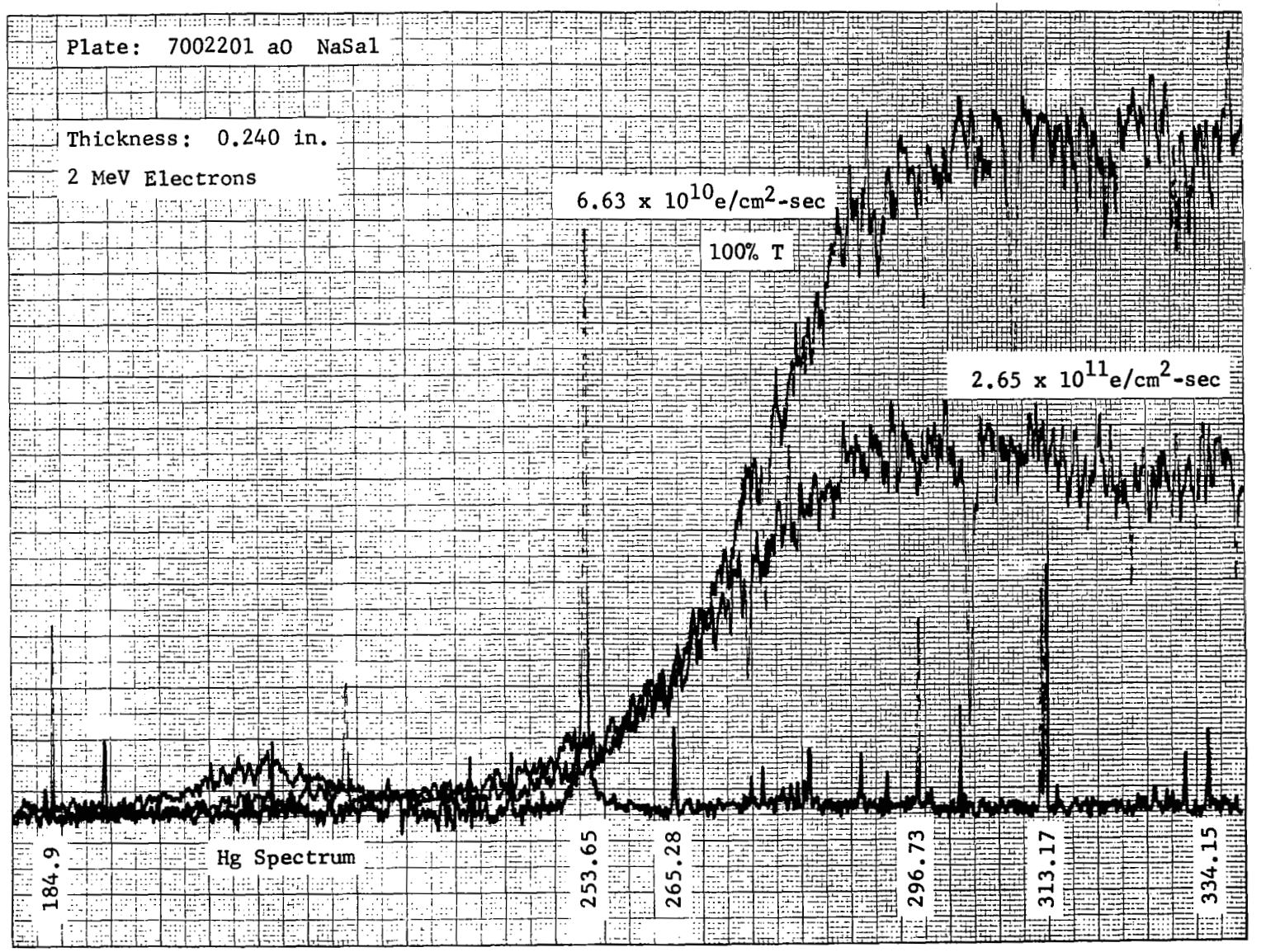

Figure 11 Electron-Induced Luminescence of UV Grade Lithium Fluoride

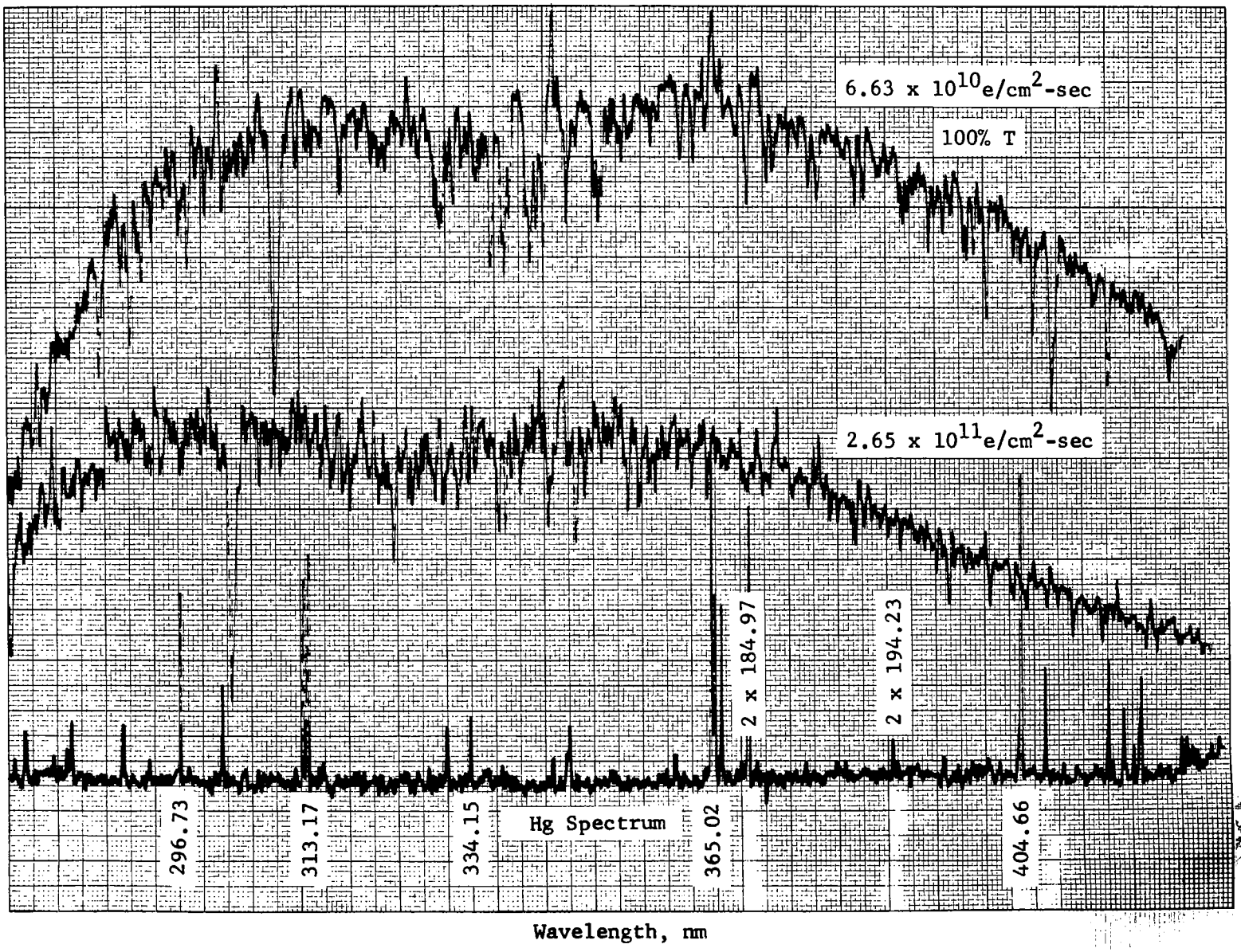

Figure 11 Electron-Induced Luminescence of UV Grade Lithium Fluoride (cont'd)

This emulsion "pitting" of Na Sal-overcoated plates is not a serious problem in data reduction. Since the majority of excursions represented by "dips" in the corresponding densitometer tracings of the pitted areas are not true density decreases they can be ignored. In any case, the pitting problem disappears at the lower photographic densities used for most of the spectrograms which are to be calibrated with the low intensity Čerenkov source.

The vendor of the spectroscopic plates indicated that the pitting problem can probably be reduced or eliminated if the final plates are pre-soaked in water before developing, and then fixed in Kodak F-5 rather than in more acid-containing Kodak Rapid Fixer which was used in fixing the preliminary plates (Ref. 29).

More serious problems than this arose when oil droplets were discovered on the jaws of the spectrographic slit and on the transfer optics mirror and when the transfer optics mirror was accidentally pitted and chipped in two unrelated incidents. Even after careful cleaning of the affected components with Freon TF after the first incident, some doubt remained as to the optical cleanliness of other components of the optical system.

Temperature Experiment

Luminescence spectra were obtained of 1/4-in.-thick Spectrosil B, thermostated at six temperatures between $-70^{\circ}F$ and $+100^{\circ}F$, and irradiated with 2 MeV electrons at a flux of $1.33 \times 10^{12} e/cm^2$-sec. The averages of the two thermocouple recordings taken before and after each of the 1 minute-duration exposures were as follows (before/after): $-64.5^{\circ}F/-65.0^{\circ}F$; $-21.5^{\circ}F/-18.0^{\circ}F$; $+19.0^{\circ}F/+19.0^{\circ}F$; $+61.5^{\circ}F/+61.5^{\circ}F$; $+82.0^{\circ}F/+82.0^{\circ}F$; and $+100^{\circ}F/+100^{\circ}F$.

The corresponding six spectrograms revealed no significant differences in spectral luminescence densities within the limits of the experimental errors involved. Evidently the temperature effect is small and cannot be discerned with the experimental procedure used.

Line Luminescence

Line luminescence was recorded for only one sample type, viz. Corning Pyrex 7740; this occurred for sample thicknesses of

1/8 in. and 1/4 in., and electron fluxes of 5.3×10^{12} and 2.65×10^{12} e/cm^2-sec, at energies of 1 and 3 MeV, respectively (see Fig. 12). It was noticed during these runs that the fixed aperture was discharging and the Faraday cup, although rotated out of the sample position, appeared to be alternately charging and discharging rapidly, as registered by Elcor current integrators connected to each. During other irradiations of Corning Pyrex 7740, e.g. 1/4 in. sample thickness, 2 MeV electron flux of 5.3×10^{13} e/cm^2-sec, no line structure was recorded on the spectrogram (see Fig. 13). In the latter case, the charging and discharging of the fixed aperture and Faraday cup did not occur. The background fogging on the 2 MeV plate due to bremsstrahlung was considerably less than that on the 1 or 3 MeV plates indicating that high electron current densities must be associated with the charging and discharging phenomenon.

A frequency analysis of the line structures observed for C 7740 shows numerous strong principal and persistent lines of atomic silicon ($\lambda\lambda$250.69, 251.61, 252.85, 288.16 and 390.55 nm); aluminum ($\lambda\lambda$309.27, 394.40, and 396.15 nm); boron ($\lambda\lambda$249.68/ 249.77 nm); lead (λ 217.00 nm); hydrogen (H_β λ486.13 nm); and carbon (λ 247.86 nm). Thus lattice line spectra and impurity line spectra are observed for this sample. These were probably excited during charging and discharging of the C 7740 sample. Some evidence of electron induced dielectric breakdown (the Lichtenberg effect) was apparent in these samples.

As in the case of a Solex sample excited by an electron beam in the earlier study (Ref. 1), the strong atomic hydrogen and carbon lines probably arise from excitation of residual hydrocarbons in the vacuum irradiation chamber, probably on the fixed beam aperture after the aforementioned oil contamination incident, or even on the sample, although each sample was cleaned with pure ethyl alcohol prior to insertion in the sample holder.

Of interest is the fact that no oxygen lines are excited in the luminescence spectrum of C 7740 although the host material is primarily SiO_2 and the silicon lines are in great evidence.

It was noted that the charging and discharging phenomenon also occurred for specimens of C 7056 and Spectrosil; however, no line luminescence was recorded in the corresponding spectrograms, at least for the preliminary plates developed at NASA/LRC.

That impurity line spectra do not appear for Spectrosil samples is indicative of the very low impurity content of these high grade optical materials. However, line spectra, both impurity

Figure 12 Electron-Induced Luminescence of Corning 7740

Figure 12 Electron-Induced Luminescence of Corning 7740 (cont'd)

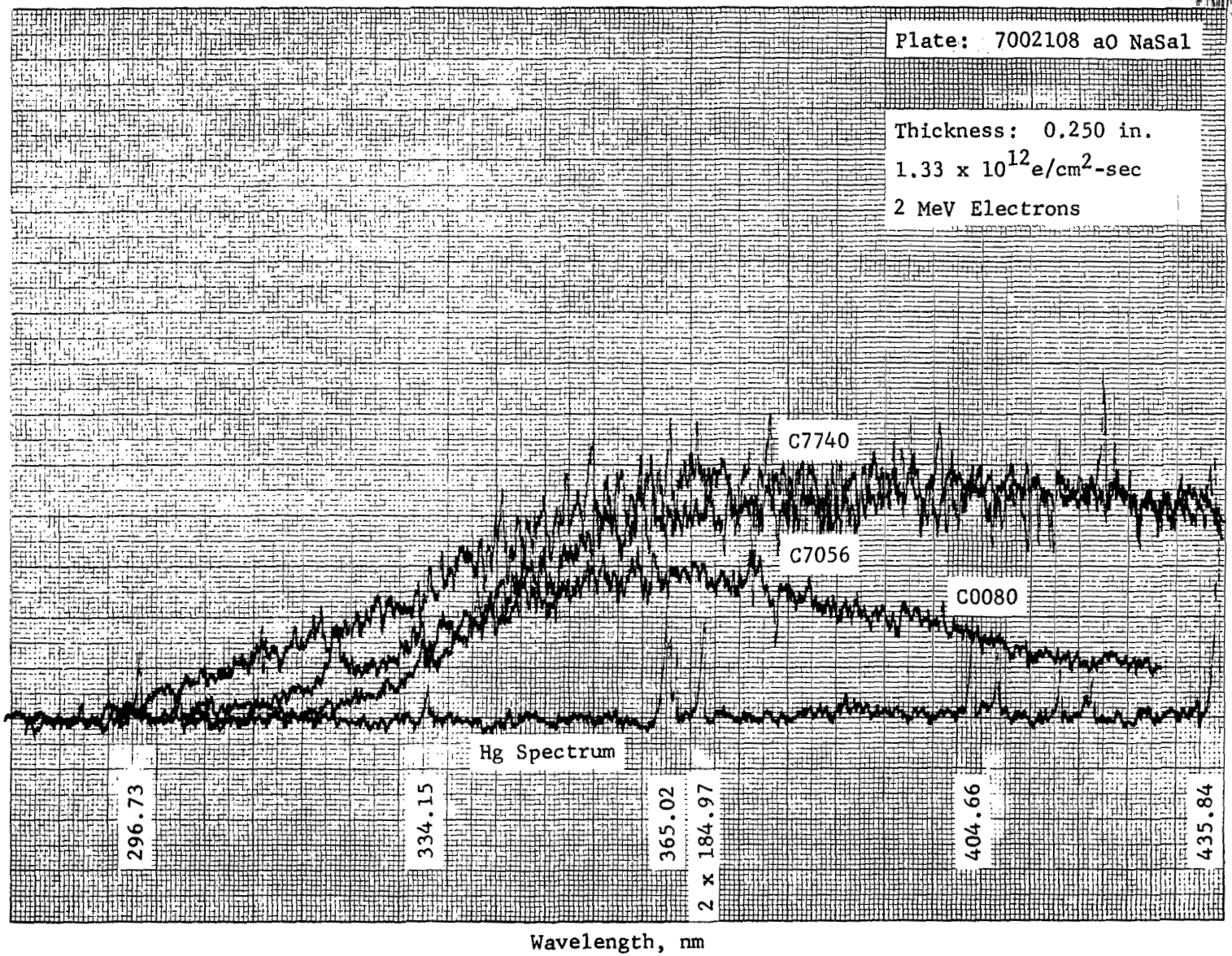

Figure 13 Electron-Induced Luminescence of Corning Glasses

and lattice spectra, in Spectrosil could be masked by the radiative de-excitation continuous spectra. The fact that the fused silica samples do not discolor upon irradiation also indicates that the samples are well annealed during production so that color center formation proceeds at a low enough rate, at least for the irradiation doses used during these experiments, that the line spectra arising therefrom are probably masked by the continuous spectra due to radiative de-excitation processes.

Continuous Luminescence

Relative densities as a function of wavelength for seven of the nine sample types (Figs. 9 through 14) were obtained from the preliminary plates developed at NASA/LRC.

Use was made of the five-step neutral density filter (transmission values: 100% T, 50% T, 25% T, 12% T and 6% T) at the saggital focus of the spectrograph to obtain a wide range of photographic (optical) densities on the spectrograms of the luminescence. Some of these are recorded in the above-referenced figures of the preliminary plates and were used in determining the optimum densities, and hence optimum electron beam and sample parameter values to be used in the final plates for good calibration and data reduction. The unlabeled tracings correspond to spectrograms obtained without the neutral density filter. Numerous equipment problems and program delays as mentioned previously, and unavailability of additional program funding to cover these, precluded calibration and data reduction of the final plates. However, some conclusions can be drawn from the preliminary plates.

Transmittance curves for most of the materials studied, some before and after electron irradiation, are presented in Figure 15 (Refs. 30 and 31) and Figures 16 through 18 (Ref. 32). Since the irradiation fluences in our program varied from 7.95×10^{13} to 1.27×10^{15} e/cm^2, these transmittance curves are of use in discussing self-absorption effects occurring in the samples, especially at the short wavelength limit. Since the intensity of luminescence as recorded on a spectrogram is dependent on many parameters, including emulsion spectral sensitivity, spectrograph and transfer optics mirror reflectivities, grating efficiency, and sample transmittance, among others, it is possible to draw only a few conclusions of a qualitative nature concerning the spectral luminescence characteristics of the samples on the basis of the spectral density and spectral transmittance curves.

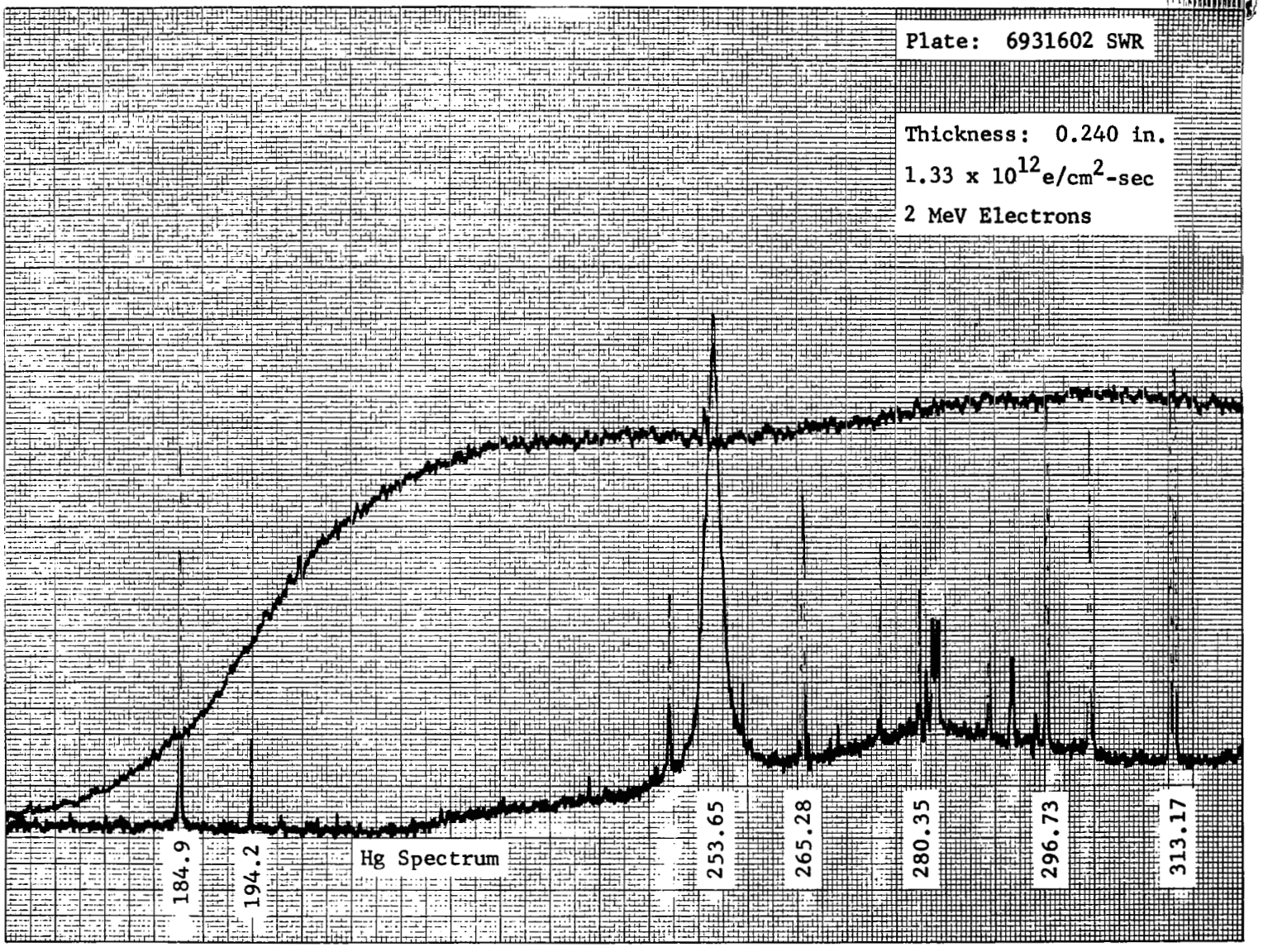

Figure 14 Electron-Induced Luminescence of UV Grade Magnesium Fluoride

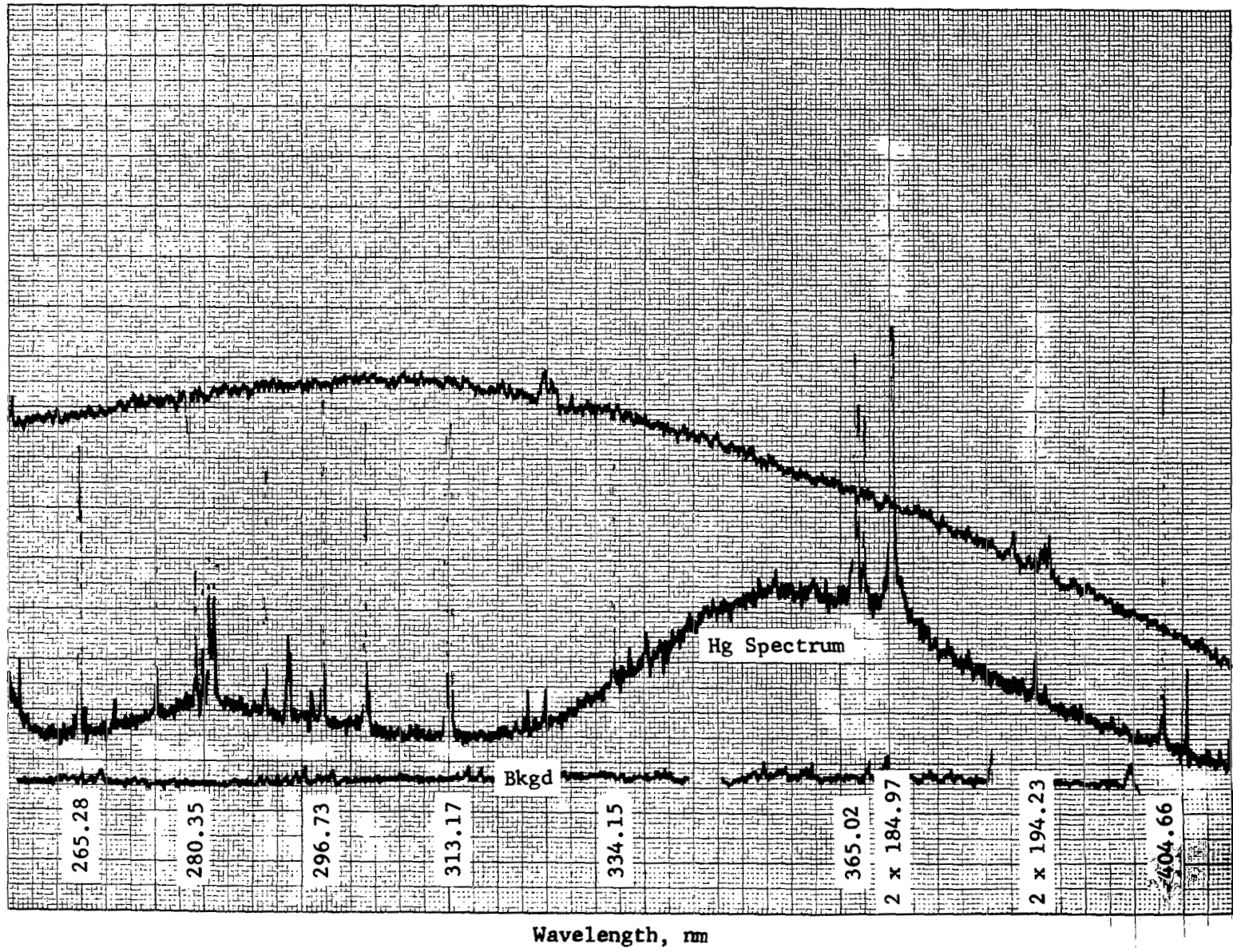

Figure 14 Electron-Induced Luminescence of UV Grade Magnesium Fluoride (cont'd)

1. uv grade sapphire
2. Spectrosil 2 mm
3. Corning 9741 0.5 mm
4. Corning 7740 3 mm
5. Corning 0080 2 mm

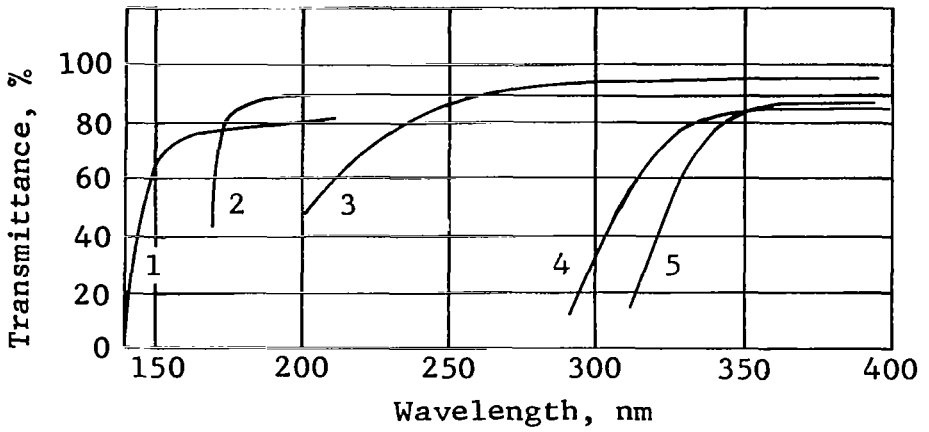

Figure 15 Transmittance of Selected Materials

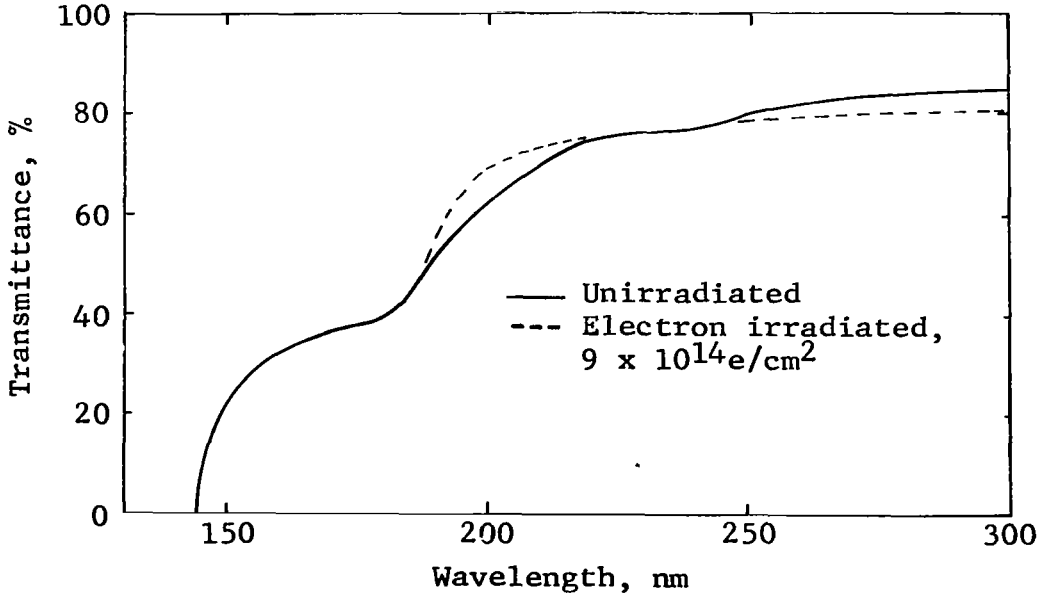

Figure 16 Transmittance of UV Grade Sapphire

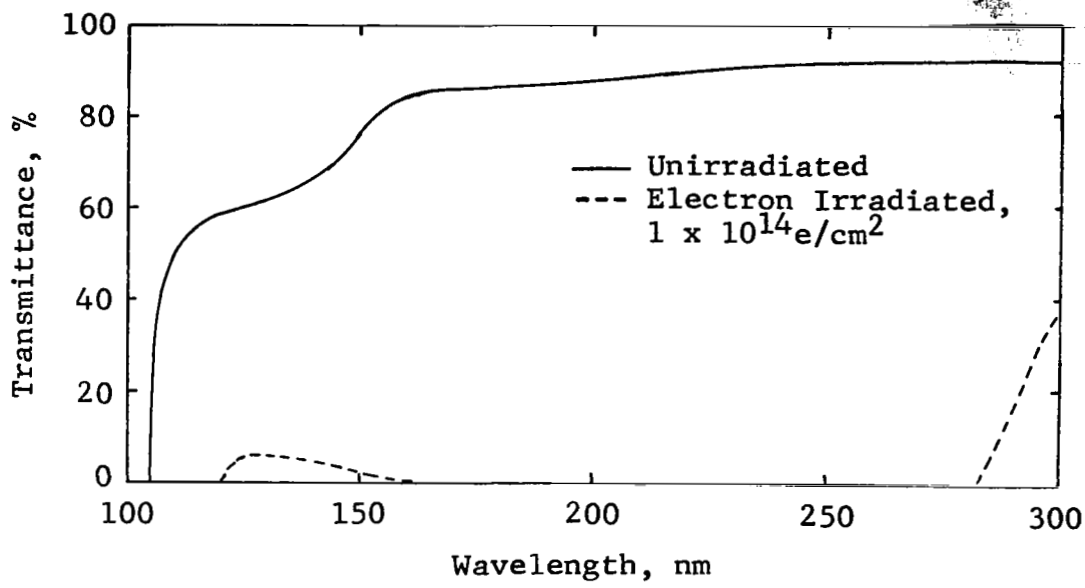

Figure 17 Transmittance of LiF

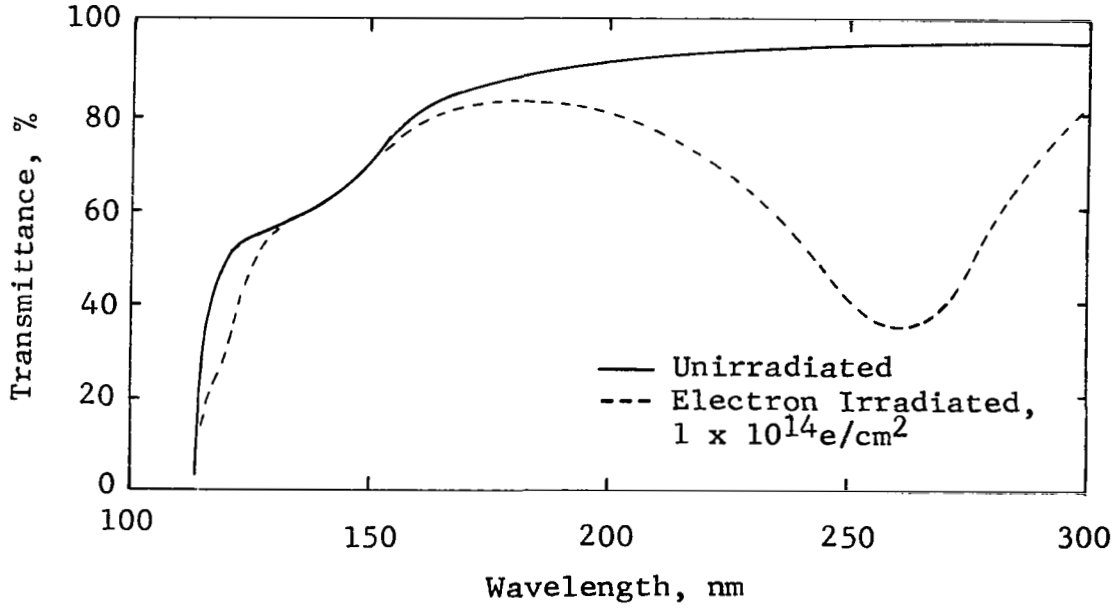

Figure 18 Transmittance of MgF_2

For Corning types 7740, 7056 and 0080, the short wavelength limits of the luminescence are approximately 285, 300, and 320 nm, respectively (Fig. 13) corresponding approximately to the transmission limits of these materials (see Fig. 15). The order of the three materials above is also the order of decreasing luminescence intensity. The densities, and hence intensities, of luminescence for C 7740 and C 7056 become approximately equal beyond 385 nm, whereas that for C 0080 decreases considerably below the two at wavelengths longer than 360 nm. The coloration of irradiated C 7740 and C 7056 was approximately the same brown tone, whereas that of C 0080 was a greenish-brown.

The uv wavelength limits of the luminescences arising from the irradiated uv transmitting materials are approximately 240, 190, 185, and 150 nm for Spectrosil B, uv grade sapphire, LiF, and MgF_2, respectively (Figs. 9, 10, 11, and 14). The corresponding uv transmission limits of these materials are 170, 145, 105, and 113 nm (Figs. 15 through 18). Some of the discrepancies between luminescence and transmittance limits can be explained by the apparent shift to longer wavelengths of the uv transmittance limit for the irradiated materials (Figs. 16 through 18). Also the grating used in these preliminary runs was blazed at 300 nm, so that the efficiency at 150 nm is low. An explanation for the luminescence dip at approximately 230 nm for irradiated LiF, and other features will have to await calibration and data reduction of the final plates.

In general, for the same electron energy and flux the luminescence density, and hence intensity, of the uv transmitting materials can be listed in decreasing order of intensity as follows: uv grade sapphire, lithium fluoride, magnesium fluoride, and the fused silicas (Spectrosil B, Suprasil II and C 9741).

Some of the uv specimens were noticeably colored by the electron irradiation: the uv grade lithium fluoride became a bright yellow, the uv grade sapphire a light beige, and the Corning 9741 a light brown. These are attributed to broad absorption bands due to color centers and can be bleached out by heating to 400°C (Ref. 32). The Spectrosil, Suprasil and uv grade magnesium fluoride samples appeared not to be colored by repeated electron fluences up to 10^{15} e/cm^2.

The above information on luminescence efficiency, uv cutoff limits and radiation-induced absorption for the various uv transmitting materials is pertinent in the final selection of the window material for the Sr^{90}-Y^{90} Čerenkov radiation source for plate calibration.

The general shapes of the luminescence density curves for Van de Graaff electron-irradiated Spectrosil (Fig. 9) and Sr^{90}-Y^{90} source-irradiated Spectrosil (Fig. 8) are quite similar in shape, with both peaking at approximately 330 nm; this is not unexpected since the incident electron energies are approximately the same in both cases, viz. 2 MeV and 2.2 MeV, respectively. The uv limit of luminescence recorded in these spectrograms is limited primarily by the spectral sensitivity of the emulsion (gelatin) of the Kodak 103aO plates in this region – viz. approximately 220 nm – which were used for convenience in these preliminary experiments.

Information on the relative contributions of the Čerenkov radiation and de-excitation radiation in the uv wavelength region, obtained from a comparison of intensities of luminescence in the 0^{o} and θ_{C} configurations, and the quantitative dependence of the luminescence intensity on such parameters as electron energy and flux, sample type and thickness, among others, will have to await calibration and data reduction of the final plates.

CONCLUSIONS

A study was conducted of the luminescence induced by 1/2, 1, 2, and 3 MeV electrons at fluxes from 6.63×10^{10} to 5.30×10^{12} e/cm^2-sec in nine optical materials, mostly of the uv transmitting types.

Both continuous and line luminescence were recorded spectrographically with an effective resolution of between 0.8 nm and 1.6 nm over the ultraviolet and near visible wavelength regions.

No temperature effect was recorded in the luminescence for 1/4-in.-thick Spectrosil B over the range -70^{o}F to $+100^{o}$F, irradiated with 2 MeV electrons at a flux of 1.33×10^{12} e/cm^2-sec.

Direct excitation of silicon, aluminum, boron and lead atoms of the Corning Pyrex C 7740 by electrons, indicated by five SiI lines, three AlI lines, one BI line and one PbI(R) line – all strong principal and/or persistent lines in their respective spectral series – are as expected from the composition of this borosilicate glass. The H_{β} and CI atomic lines are attributed to electron excitation of traces of oil in the system.

Atomic lines in the electron-irradiated fused silica and uv grade sapphire are probably obscured by the more intense continuous luminescence.

Experimental difficulties with the equipment and contamination problems concerning the fabrication of a Sr^{90}-Y^{90} Čerenkov source for plate calibration resulted in numerous program delays; these, coupled with program funding problems, precluded calibration and data reduction of some forty final plates.

Analysis of the relative density tracings of some of the preliminary plates on seven of the nine sample types yields the following qualitative conclusions. The materials, in order of decreasing intensity of continuous luminescence induced by electrons of a particular energy and flux, are as follows: uv grade sapphire, lithium fluoride, magnesium fluoride, and the fused silicas (Spectrosil B, Suprasil II, and C 7941), and Corning types C 7740, C 7056 and C 0080. The short wavelength limit of the luminescence generally approached the short wavelength transmission limit of the material modified by electron-induced absorption and sample thickness.

The quantitative dependence of the continuous luminescence intensity on such parameters as electron energy and flux, sample type and thickness, among others, and the relative intensities of the Čerenkov and de-excitation radiation components await calibration and data reduction of the final plates.

A 38 Ci Sr^{90}-Y^{90} Čerenkov radiation source designed and constructed in this program and calibrated at one wavelength, can be used for calibration of the final plates using revised procedures concerning weak light sources as specified herein.

RECOMMENDATIONS

Three main recommendations are indicated. First, funding should be provided to complete the ultraviolet luminescence program. This would involve calibration of the forty spectroscopic plates containing the luminescence spectrograms using the Sr^{90}-Y^{90} Čerenkov uv radiation source and/or tungsten-iodine irradiance standard, and subsequent data reduction thereof using the IBM-360 digital computer program.

Data thereby obtained, expressed in units of nW/cm^2-ster-nm versus wavelength at resolutions of 0.8 nm and 1.6 nm, would be used to determine the dependence of the continuous luminescence on such parameters as sample type and thickness, electron energy and flux, and on the relative contributions of the Čerenkov and de-excitation radiation components.

Second, the proton irradiation-luminescence experiments should be conducted to complement the corresponding electron irradiation-luminescence experiments conducted under the present program in the uv region, and to supplement the data on proton-induced luminescence obtained in the earlier program (Ref. 1).

Finally, this program should be expanded to cover the infrared region; the last wavelength region of interest in this general technology program involving indigenous space radiation effects on optical materials of scientific instruments.

Continuous luminescence radiation will be generated by charged particles in infrared transmitting materials of infrared spectrometers and radiometers used in atmospheric dynamics and energy balance studies, temperature mapping and temperature sounding of surfaces and atmospheres of planetary bodies. Infrared components of interest include germanium objective lenses, the irtran series of field lenses, silicon detectors, and various infrared beamsplitters, compensating plates and interference filters of corresponding interferometer (Fourier) spectrometers and multiple infrared radiometers.

Of the continuous luminescence radiation generated in infrared transmitting materials, de-excitation radiation will probably account for a major part thereof. Čerenkov radiation will also be generated in infrared transmitting materials in the infrared wavelength region as long as the dielectric constant ϵ is greater than β^{-2}. The contribution of the total luminescence to the response of the infrared detectors downstream from the infrared transmitting optics must be known if meaningful quantitative measurements are to be made of the infrared field under observation. Although some data have been obtained on electron- and proton-induced infrared radioluminescence of some infrared optical materials, the measurements were made using photoconductive detectors in conjunction with a series of broad-band-pass filters yielding data on integrated intensities over only four quite broad wavelength regions for only a relatively few number of infrared materials of interest to current space programs (Refs. 4 and 5).

The techniques developed for NASA/LRC under Contract NAS1-7734 for the visible and ultraviolet wavelength regions can be easily adapted to permit measurements in the infrared wavelength region to 16,000 nm.

APPENDIX A

FEASIBILITY STUDIES: ČERENKOV SOURCE

The requirements for the ultraviolet radiation source were that the radiation be a continuum extending from the lithium fluoride cutoff into the near visible, that its spectral intensity be comparable to that of the observed Van de Graaff electron-induced luminescence, and that it be stable over long periods. A logical choice was a Čerenkov radiation source. The theory and calculations in support of this choice are presented below.

Theory

Light emission from this phenomenon was first reported by Čerenkov (Refs. 33 and 34) who demonstrated that fast electrons passing through transparent media result in the emission of light in a continuum extending from the visible into the ultraviolet. A classical theory of this effect was developed by Frank and Tamm (Ref. 19). The emission was shown to result from the interaction between a charged particle whose velocity is greater than the phase velocity of light in the medium and the dielectric field of the medium. The theory yields the following expression for the number of photons, N_E, with wavelengths between λ_1 and λ_2 emitted along the path of a charged particle of initial energy, E:

$$N_E = 2\pi\alpha\left(\frac{1}{\lambda_2} - \frac{1}{\lambda_1}\right)\int_{\beta}^{\frac{1}{n}} \left(1 - \frac{1}{\beta^2 n^2}\right) d\ell \qquad (1)$$

where α = fine structure constant, $\sim \frac{1}{137}$

β = ratio of the velocity of the particle to the speed of light

n = refractive index of the medium for the emitted light, and

ℓ = path length of particle within the medium.

The light is emitted in a hollow cone about the direction of the particle with a characteristic apex angle, 2 θ, defined by

$$\cos\theta = \frac{1}{\beta n} . \qquad (2)$$

This angle decreases as the particle energy degrades in its passage through the medium, and light emission ceases when the particle velocity reaches 1/n.

If the charged particles have a distribution of energies, then the factor p_E, the probability of a particle energy between E and E + dE, must be included in the integral in Equation (1). Belcher (Refs. 35 and 36) and Anderson (Ref. 36) have presented theoretical and experimental results for Čerenkov emission from several radioisotopes in aqueous solution. Of particular interest are their data for three pure-beta emitters: Tl^{204}, P^{32}, and Sr^{90}-Y^{90} in secular equilibrium. Pure-beta emitters are the most desirable since the efficiency for Čerenkov emission by betas is greater than that for other types of radiation and the radiation hazards are less. Sr^{90}-Y^{90} was found to be a particularly desirable particle source since it produces 47 quanta between 300 nm and 700 nm per disintegration and has a half-life of 27.7 years.

Intensity Calculations

Calculations were performed to determine the absolute intensity of the Čerenkov radiation in the mid-uv from an aqueous solution of Sr^{90}-Y^{90}. Two assumptions were made in these calculations:

(1) That the betas suffered no number loss in the slowing-down process from either absorption or escape from the vessel;

(2) That the medium and the vessel do not absorb the emitted Čerenkov radiation.

The Sr^{90}-Y^{90} beta spectrum of Mears and Cole (Ref. 37), normalized to one disintegration, was used in the calculations. This spectrum was divided into increments of 0.1 MeV and integrated over each interval. The contribution of each of these intervals by both primary and degraded betas to the photon emission in a one nm interval about 215 nm was then computed. A photon output of 0.92 photons/dis was obtained. When extended to the 300-700 nm range, an output of 80 photons/dis was obtained. This value compares favorably with the Anderson and Belcher (Ref. 36) data of 47 photons/dis over the same range in which particle number losses and escapes were included.

For purposes of comparison, typical luminescence intensities encountered in experimental irradiations of optical materials were calculated from data obtained in the earlier program (Ref. 1). Soda lime glass irradiated with 1 MeV electrons at a flux of 2.5×10^{12} e/cm^2-sec exhibited an intensity of 1.5×10^{1} nwatt/ster-nm at 403 nm. Spectrosil irradiated with 3 MeV electrons at 1.3×10^{12} e/cm^2-sec exhibited an intensity of 4.2×10^{2} nwatt/ster-nm at 362 nm. The calculated value for an aqueous solution of Sr^{90}-Y^{90} of 0.92 photon/dis-nm at 215 nm extrapolates to 5.2×10^{-4} nW/mCi-ster-nm at 362 nm and 3.7×10^{-4} nW/mCi-ster-nm at 403 nm. Thus approximately 40 Ci of Sr^{90}-Y^{90} would be required to obtain a source luminescence equal to that of soda lime and 800 Ci to equal that of Spectrosil at the wavelengths cited.

Source intensities of this magnitude present several problems. Anderson and Belcher (Ref. 36) reported non-linearity of luminescence with specific activity of Sr^{90}-Y^{90} sources in the μCi/mℓ range. Specific activities of kCi/mℓ probably cannot be attained because of solubility problems. The radiation hazards and handling problems, particularly for a liquid source, are severe.

Some of these difficulties can be overcome by use of a solid, rather than liquid, beta source. In this concept, betas would pass from the source through a thin window into the luminescing medium. This arrangement overcomes problems of impurities, nonlinearity, specific activity, and particle escape, and alleviates the handling problem to some extent.

It was tentatively concluded from an examination of the luminescence data in Reference 1 that the light emitted from the electron-irradiated fused silica specimens was primarily Čerenkov radiation. This conclusion is substantiated by two observations: the observed energy per unit wavelength of the radiation in the low visible and near uv region appears to follow the $1/\lambda^3$ distribution predicted for Čerenkov radiation by Frank and Tamm (Ref. 19) and the calculated intensity of Čerenkov radiation emitted at 400 nm by fused silica irradiated with 1 MeV electrons is comparable to that observed in Reference 1. A possible Čerenkov radiation source could therefore consist of a thin-window Sr^{90}-Y^{90} source utilizing uv-grade fused silica as a medium.

Calculations were therefore performed to determine the Čerenkov output at 200 nm from Sr^{90}-Y^{90} betas in silica. The necessary assumptions have been previously described. An output of 0.63 photons per disintegration was obtained. This is

equivalent to 1.8×10^{-3} nW/mCi-ster-nm if a 4π distribution is assumed. This intensity extrapolates to 3.0×10^{-4} nW/mCi-ster-nm at 362 nm. As previously mentioned, Spectrosil irradiated with 3 MeV electrons at a flux of 1.3×10^{12} e/cm^2-sec exhibited a light output of 4.2×10^{2} nW/ster-nm at 362 nm. Thus a beta source intensity of approximately 1400 Ci would be required to produce a Čerenkov output equal to that of Spectrosil at 362 nm irradiated under the described conditions. The light output at 403 nm from soda lime glass irradiated with 1 MeV electrons at a flux of 2.5×10^{12} e/cm^2-sec was 1.5×10^{1} nW/ster-nm. Extrapolation of the calculated value for Sr^{90}-Y^{90} betas incident on fused silica yields an intensity of 2.2×10^{-4} nW/mCi-ster-nm at 403 nm. Thus a 70 Ci source would be required to produce Čerenkov radiation equal to that of soda lime glass at 403 nm irradiated under the described conditions.

A Sr^{90}-Y^{90} source strength of the order of 1000 Ci would therefore be required to obtain Čerenkov radiation with an intensity approximating that observed in electron-irradiated Spectrosil. This is a minimum since light intensities at least 50 times higher than those previously discussed for soda lime were observed in fused silicas irradiated at higher electron energies and fluxes.

The above calculations for a Čerenkov uv source were subsequently refined by three major modifications:

(1) Self-attenuation of the radioisotope source was taken into consideration.

(2) Extended source calculations were performed to correct for the finite size and proximity of the source and absorbing medium.

(3) Directionality of the Čerenkov radiation was factored into the calculations.

The maximum feasible strength of a Sr^{90}-Y^{90} beta source was calculated. The source was assumed to consist of $SrTiO_3$ with a specific activity of 60 Ci/gm and density of 3.93 gm/cm^3; these data are nominal values obtained from Reference 38. The source container was assumed to consist of stainless steel with a 10-mil window. The maximum thickness of the source material was defined as that thickness which, together with the 10-mil window, attenuates the highest-energy betas of Sr^{90}-Y^{90}, 2.2 MeV, to an energy of 0.3 MeV, the Čerenkov cutoff energy in fused silica.

A maximum thickness of source material of 0.3 cm was obtained. The maximum source strength per unit surface area was thus 71 Ci/cm^2.

The self-attenuation of a Sr^{90}-Y^{90} source 0.3-cm thick with a 10-mil stainless steel window was then calculated. The source was considered to be divided into ten layers of equal thickness, and the energy attenuation of Sr^{90}-Y^{90} betas from each layer passing through the remaining layers and window was calculated. The assumptions of no number losses of betas, and perpendicular passage through the source material were made. Since the original Sr^{90}-Y^{90} beta spectrum was normalized to one disintegration, the resultant of this calculation was an attenuated beta spectrum normalized to one disintegration of unattenuated activity.

The theory of Frank and Tamm (Ref. 19) was then used to calculate the Čerenkov radiation output of betas with this attenuated spectrum incident on fused silica. A Čerenkov output of 0.11 photons/dis-nm at 200 nm was obtained.

An output of 0.63 photons/dis-nm had been calculated previously for the unattenuated betas of Sr^{90}-Y^{90} on fused silica. An output of 0.16 photon/dis-nm would be expected from the effective loss of betas attenuated to energies less than 0.3 MeV. The lower output of the attenuated betas reflects the significant energy degradation of the self-attenuated Sr^{90}-Y^{90} beta spectrum.

The above resultwas then applied to a reasonable source-to-fused silica configuration in order to calculate a Čerenkov output for a practical situation. A Sr^{90}-Y^{90} source 1.5 cm in diameter and 0.3 cm thick with a 10-mil window was assumed. Total strength of this source would be approximately 130 Ci. Standard techniques (Ref. 39) were used to calculate the flux of unattenuated betas from such a source through a 0.6 cm diameter area placed 0.3 cm from, parallel to, and coaxial with the source. A flux value of 7.6×10^{11} e/cm^2-sec was obtained.

When this result is applied to the previously calculated Čerenkov output per disintegration, the Čerenkov source steradiancy would be 1.6 nW/cm^2-ster-nm at 400 nm if uv uniformity over 2π is assumed. A typical experimental value (Ref. 1) for the steradiancy of fused silica irradiated with electrons is 36 nW/cm^2-ster-nm at 400 nm for 3 MeV electrons incident on quartz at 2.5×10^{12} e/cm^2-sec. Intensity of the Čerenkov uv source would thus be at least 20 times too low.

The source would be too intense, however, for the second proposed application: the calibration of photomultipliers used in star trackers. The irradiance of a zero magnitude star (Ref. 40) is approximately 8 x 10^{-6} nW/cm^2-nm at its peak near 380 nm. The irradiance at 30 cm from a 1 cm^2 source in the previously described configuration is 1.8 x 10^{-3} nW/cm^2-nm at 400 nm, a factor of approximately 200 higher than desired.

The accuracy of the Čerenkov calculation was checked by comparing experimental values for 3 MeV electrons incident on fused silica with a calculated value under the given experimental conditions. This comparison had been made previously with the assumption of a 4π distribution.

The directionality of the Čerenkov light was considered in the present comparison. Some unpublished data on the Čerenkov light emitted at angles of 0^o, 45^o, and 90^o from a 3 MeV electron beam incident on fused silica were used for this purpose. It was assumed that the light output was symmetrical in the forward direction, and extrapolations were made in the backward direction. A correction factor for Čerenkov calculations at 3 MeV was derived by dividing the steradiancy at 0^o by the spherical integral of the experimentally observed steradiancy. The Čerenkov output in the forward direction per steradian was found to be approximately 0.13 of the total output.

This factor was applied to the calculation of 100 nA of 3 MeV electrons incident on fused silica and a steradiancy of 1.4 x 10^2 nW/cm^2-ster-nm at 400 nm was obtained in the forward direction. This is a factor of 4 higher than the measured value of 36 nW/cm^2-ster-nm. The source of this discrepancy is not known, since good agreement between calculated and measured values was expected for the simple geometry of this problem.

The intensity of the maximum feasible Čerenkov source (130 Ci of Sr^{90}-Y^{90}) would thus appear to be 20-100 times lower than needed for calibration of spectroscopic plates under the experimental conditions used in Reference 1 and approximately 200 times higher than that desired for calibration of photomultipliers.

An investigation into the techniques of fabricating Sr^{90} sources revealed that ORNL, for one, uses microspheres of strontium titanate in which the voids are initially filled with molten aluminum, thereby forming a unified source. In this configuration the maximum practical source intensity is about 50 Ci of Sr^{90}.

The use of revised procedures of recording the luminescence at lower densities and development of a modified plate calibration technique using a low intensity irradiance standard are discussed earlier. The procedures permit effective use of a nominal 50 Ci Sr^{90}-Y^{90} Čerenkov uv radiation source in spectroscopic plate calibrations.

Radioactive Source Hazard

The 38 Ci Sr^{90}-Y^{90} source is hazardous and safe storage and handling procedures must be exercised.

The source (Fig. 5) consists of a stainless steel capsule containing microspheres of strontium titanate in an aluminum matrix. The active volume is approximately 0.59 in. in diameter by 0.12 in. deep. The capsule is 0.82 in. in diameter by 0.56 in. high with a recessed 0.010-in. thick stainless steel window at one end adjacent to the source. The thin window permits beta particle transmission to a transparent dielectric material for generation of Čerenkov radiation.

Strontium-90 and yttrium-90 are in secular equilibrium, since Sr^{90} decays by beta emission with a 27.7 year half-life to Y^{90}, which in turn decays by beta emission to Zr^{90}, which is stable. Beta end-point energies are 546 keV for Sr^{90} and 2.27 MeV for Y^{90}. Estimates of the attenuation of the activity by the source matrix and window indicate that less than 10% of the Y^{90} betas are transmitted through the window.

Measurements of the source beta dose rate were made using LiF thermoluminescence dosimeters which were especially suitable for such determinations (Ref. 41). A value of 1300 rad/hr was measured at one foot from the window which is 50% higher than the dose rate calculated using a classical formula.

A beta dose rate of 1300 rad/hr (0.36 rad/sec) at 1 foot is equivalent to a whole body dose if received by the lens of the eye. Viewing the source directly without the benefit of transparent shielding would probably result in an overexposure (1.25 rem/quarter). The use of transparent shielding is mandatory when handling the source.

Bremsstrahlung radiation from total absorption of the beta radiation amounts to approximately 120 mR/hr-Ci at 1 foot (Ref. 42) or 4.5 R/hr at 1 foot for the 38 Ci source. The average bremsstrahlung dose was 3.2 R/hr as measured with a

Radector at 1 foot from the side of the source. In this direction the betas are completely absorbed and the bremsstrahlung is somewhat attenuated.

Other monitoring instruments will give widely varying responses when exposed to the window side of the source. The results of such measurements must be interpreted carefully.

The source is currently stored in the steel and lead container (Fig. 6) described earlier. Dose rate measurements at the top and sides of the closed container are approximately 2 and 1 mR/hr, respectively.

REFERENCES

1. "Spectrographic Studies of Luminescence in Charged-Particle-Irradiated Optical Materials," General Dynamics Fort Worth Division Report FZK-364, NASA CR-66758 (21 March 1969).

2. Code, A. D., et al, "Ultraviolet Photometry from the Orbiting Astronomical Observatory. I. Instrumentation and Operation," Astrophysical J., 161 (August 1970), pp. 377-388.

3. Jelley, J. V., Čerenkov Radiation, Pergammon Press, New York (1958), p. 22.

4. Downing, R. G., Snively, F. T., and Van Atta, W. K., "Investigation of Charged Particle Effects on Infrared Optical Materials," AFML-TR-65-261, Wright-Patterson AFB (November 1965).

5. Downing, R. G., Snively, F. T., and Van Atta, W. K., "Investigation of Charged Particle Effects on Infrared Optical Materials, Part II," AFML-TR-66-224, Wright-Patterson AFB (August 1966).

6. A Study of Jupiter Flyby Missions, Final Technical Report, General Dynamics Fort Worth Division Report FZM-4625 (17 May 1966), p. 3-186.

7. Zagorites, H. A., and Lee, D. Y., "Gamma and X-ray Effects in Multiplier Phototubes," IEEE Trans. Nuc. Sci. Ns-12 (1965), p. 343.

8. Favale, A. J., Kuehne, F. J., and D'Agostino, M. D., "Electron Induced Noise in Star Tracker Photomultiplier Tubes," IEEE Trans. Nuc. Sci. NS-14, No. 6 (1967), p. 190.

9. Reed, E. I., Fowler, W. B. Aitken, C. W., and Brun, J. F., "Some Effects of MeV Electrons on the OGO-II (POGO) Airglow Photometers," NASA TM X-55791, Goddard Space Flight Center (March 1967).

10. Op. cit., Ref. 1, Appendix A, p. 122.

REFERENCES (Cont'd)

11. Compton, D. M. J., Bryant, J. F., and Cesena, R. A., "Mechanisms of Optical Emission from Ruby Excited by Short Pulses of Relativistic Electrons," Physics of Quantum Electronics, Conference Proceedings, P. L. Kelley, B. Lax, and P. E. Tannenwald (eds.), McGraw-Hill Book Co., Inc., New York (1966), p. 305.

12. Mitchell, E. W. J., and Townsend, P. D., "The Luminescence from Ruby Excited by Fast Electrons," Proc. Phys. Soc. (London), 81 (1963), p. 12.

13. de Figueiredo, R. P., "On Fast Electron Pumping of Ruby," Quantum Electronics, Proceedings of the Third International Congress, P. Grivet and N. Bloembergen (eds.), Columbia, New York (1964), p. 1353.

14. Low, W., Appl. Phys. Letters, 5 (1964), p. 35.

15. Collins, G. B., and Reiling, V. G., "Čerenkov Radiation," Phys. Rev., 54 (1938), p. 499.

16. Čerenkov, P. A., "The Spectrum of Visible Radiation Produced by Fast Electrons," Comptes Rendus (Doklady) Acad. Sci. URSS, 20, No. 9 (1938), p. 651.

17. Greenfield, M. A., Norman, A., Dowdy, A. H., and Kratz, P. M., "Beta- and Gamma-Induced Čerenkov Radiation in Water," J. Opt. Soc. Amer., 43, No. 1 (1953), p. 42.

18. Rich, J. A., Slovacek, R. E., and Struder, F. J., "Čerenkov Radiation from a Co^{60} Source in Water," J. Opt. Soc. Amer., 43, No. 9 (1953), p. 750.

19. Frank, C. R., and Tamm, I. E., Comptes Rendus Acad. Sci. URSS, 14, No. 3 (1937), p. 109.

20. Kodak Plates and Films for Science and Industry, Kodak Publication No. P-9, Eastman Kodak Co., Rochester, N. Y. (1967).

21. Sawyer, R. A., Experimental Spectroscopy, Dover Publications, Inc., New York, 3rd ed. (1963), pp. 254-287.

22. Ibid., p. 203.

REFERENCES (Cont'd)

23. Chizhikova, Z. A., "Luminescence and Vavilov-Cherenkov Radiation in Solutions Bombarded by Gamma Rays," Optics and Spectroscopy, VII, No. 2 (1959), p. 141.

24. Catalog No. 5, ICN Chemical and Radioisotope Division, International Chemical and Nuclear Corp., Irvine, Calif.

25. Op. cit., Ref. 21, p. 276.

26. Allison, R., and Burns, J., "Ultraviolet Sensitization of Photographic Plates with Sodium Salicylate," J. Opt. Soc. Am. 55 (1965), p. 574.

27. Allison, R., Burns, J., and Tuzzolino, A. J., "Absolute Fluoresence Quantum Efficiency of Sodium Salicylate," J. Opt. Soc. Am. 54 (1964), p. 747.

28. Allison, R., Burns, J., and Tuzzolino, A. J., "Stability of Fluorescence of Sodium Salicylate," J. Opt. Soc. Am. 54 (1964), p. 1381.

29. Hahn, E. J., Scientific Photography Markets, Eastman Kodak Company, Rochester, New York, private communication (January 1970).

30. "EMI Photomultiplier Preferred Tube Type Chart," Whittaker Corp., Jencom Div., Plainview, L. I., N. Y.

31. "Linde Optical Grade Sapphire," Linde Crystal Products Bulletin F-917-D, Union Carbide Corporation, Linde Division, East Chicago, Ind.

32. Heath, D. F., and Sacher, P. A., "Effects of a Simulated High-Energy Space Environment on the Ultraviolet Transmittance of Optical Materials Between 1050 Å and 3000 Å," Applied Optics 5 (June 1966), pp. 937-943.

33. Čerenkov, P. A., C. R. Acad. Sci. URSS 2 (1934), p. 451.

34. Čerenkov, P. A., Phy. Rev. 52 (1937), p. 378.

35. Belcher, E. H., Proc. Roy. Soc. A 216 (1953), p. 90.

36. Anderson, W., and Belcher, E. H., Brit. J. Appl. Phys 5 (1954), p. 53.

37. Mears, K. E., and Cole, W. M., Lockheed Aircraft Co., Georgia Division, Report NR-73 (1959).

38. Arnold, E. D., "Handbook of Shielding Requirements and Radiation Characteristics of Isotopic Power Sources for Terrestrial, Marine, and Space Applications," ORNL-3576 (April 1964).

39. Handbook of Mathematical Tables, Weast, Robert C., Editor in Chief, The Chemical Rubber Co. (1964).

40. Draper, L. T., "Star Tracker Calibration," NASA TN D-4594 (June 1968).

41. Kastner, J., Hukkoo, R., and Oltman, B. G., "Lithium Fluoride Thermoluminescent Dosimetry for Beta Rays," in Luminescence Dosimetry, AEC Symposium Series 8, Frank H. Attix, ed., Report No. CONF-650637, USAEC, Oak Ridge, Tenn. (April 1967), pp. 482-489.

42. Los Alamos Handbook of Radiation Monitoring, LA-1835 (3d ed.), Los Alamos Scientific Laboratory, Los Alamos, New Mexico (November 1958), pp. 134, 137.

43. Ibid., p. 134.

UNCITED REFERENCES

1. Zrelov, V. P., Cherenkov Radiation in High-Energy Physics, Parts I and II, AEC-Tr-7099 UC-34 TT70-50003, Ketter Press, Jerusalem (1970).

NASA-Langley, 1971 —— 23 CR-1921